PARTICLE SIMULATION OF THE LOW-α PIERCE DIODE

by

T. L. Crystal and S. Kuhn

Memorandum No. UCB/ERL M84/74

20 September 1984

cover

PARTICLE SIMULATION OF THE LOW-α PIERCE DIODE

by

T. L. Crystal, and S. Kuhn

Memorandum No. UCB/ERL M84/74

20 September 1984

ELECTRONICS RESEARCH LABORATORY

College of Engineering
University of California, Berkeley
94720

Title page

PARTICLE SIMULATIONS OF THE LOW-α PIERCE DIODE

T.L. Crystal and S. Kuhn[a)]

ERL, University of California, Berkeley, CA 94720

The evolution of small initial perturbations of the uniform equilibrium of the "classical" Pierce diode [J. Pierce, J. Appl. Phys. 15, 721 (1944)] is studied using particle simulations. These simulations have been performed with the new bounded-plasma code PDW1 and cover the parameter range $0 < \alpha < 3\pi$, where $\alpha = \omega_p L/v_o$. In the linear regime, three stages (initial-transit, adjustment, and dominant-eigenmode) are distinguished; oscillation frequencies, growth/damping rates, and potential profiles of the dominant eigenmode as well as oscillation frequencies of the next-to-dominant eigenmode are recovered and shown to agree quantitatively with recent analytical results. In the linearly unstable cases, the system evolves nonlinearly to a final state which may be either a new, nonuniform d.c. equilibrium, or a state of large-amplitude oscillations. In particular, for $\alpha = 1.5\pi$ the character of the final state is found to depend on the details of the initial conditions.

a) Permanent address: Institute for Theoretical Physics, University of Innsbruck, A-6020 Innsbruck, Austria.

I. INTRODUCTION AND SUMMARY

The "classical" Pierce diode[1] is a special 1-d configuration with boundaries defined by two equipotential (short-circuited) planar electrodes separated some distance L, enclosing a spatially uniform ion background of rigid ($m_i \to \infty$) ions, and having a cold electron beam injected at some velocity v_o from the left hand electrode. Electrons hitting either electrode are absorbed; the uniform beam injection provides a constant injected current density $J_o = -en_o v_o$. The classical Pierce diode has proven to be fundamentally useful as an archetypical bounded-plasma system, capable of exhibiting important boundary-dominated physics, e.g. formation of virtual cathodes (steady and oscillating), strong double-layers, and sheaths; as such, it has been heavily studied both analytically[1-5] and more recently with simulations[4,6]. Similar "Pierce type" configurations have been used to model many devices including collective effects accelerators[7], inertial confinement fusion drivers[8], Q-machines[9], and high-power microwave sources[10]. Thus the classical Pierce diode is of both fundamental and applied interest and, in fact, represents a "gauge" case against which more or less modified configurations are conveniently compared. A complete analytical theory of the linear Pierce instability has been given recently[5] providing detailed predictions of the time evolution of any small amplitude (linear) perturbation, in terms of the system eigenfrequencies and eigenmode profiles.

I. INTRODUCTION AND SUMMARY

The "classical" Pierce diode[1] is a special 1-d configuration with boundaries defined by two equipotential (short-circuited) planar electrodes separated some distance L, enclosing a spatially uniform ion background of rigid ($m_i \to \infty$) ions, and having a cold electron beam injected at some velocity v_o from the left hand electrode. Electrons hitting either electrode are absorbed; the uniform beam injection provides a constant injected current density $J_o = -en_o v_o$. The classical Pierce diode has proven to be fundamentally useful as an archetypical bounded-plasma system, capable of exhibiting important boundary-dominated physics, e.g. formation of virtual cathodes (steady and oscillating), strong double-layers, and sheaths; as such, it has been heavily studied both analytically[1-5] and more recently with simulations[4,6]. Similar "Pierce type" configurations have been used to model many devices including collective effects accelerators[7], inertial confinement fusion drivers[8], Q-machines[9], and high-power microwave sources[10]. Thus the classical Pierce diode is of both fundamental and applied interest and, in fact, represents a "gauge" case against which more or less modified configurations are conveniently compared. A complete analytical theory of the linear Pierce instability has been given recently[5] providing detailed predictions of the time evolution of any small amplitude (linear) perturbation, in terms of the system eigenfrequencies and eigenmode profiles.

In the present paper we are concerned with particle simulations of the perturbed uniform classical Pierce diode. In the linear regime, which is our main concern here, quantitative comparisons with the analytical and numerical results given in Ref. 5 show that there is detailed agreement between theory and simulations. For the unstable cases, the transition from the linear into the nonlinear regime is observed; it is found that the final (i.e., time-asymptotic) state may be either d.c. or oscillatory, and may depend on the initial conditions.

The particular d.c. equilibrium ($\partial/\partial t = 0$) considered by Pierce[1] for his classical diode model postulated a uniform system, i.e., one in which $n_e(x) = n_i(x) = n_o$ and $\phi(x) = \text{const}$. The assumption of infinite ion mass physically prevents the ion-electron "two-stream" interaction in the plasma. In the infinite-plasma approximation, the equilibrium medium's dispersion relation is simply (Ref. 11, p. 137) $\varepsilon \equiv 1 - \omega_p^2/(\omega - kv_o)^2 = 0$; this medium's stability is shown analytically in that for all real k, the frequencies ω returned by the dispersion relation are also real. Using a fluid formalism for the plasma and imposing both the particle boundary conditions (i.e., the electron injection and absorption) and the external circuit requirements (i.e., the short-circuit: $\phi(x=0) = \phi(x=L)$ on the uniform "classical" diode, Pierce[1] obtained the transcendental characteristic equation or "dispersion relation" for the perturbation eigenfrequencies:

$$\frac{\omega+\omega_p}{\omega-\omega_p}\frac{\omega}{\omega_p}\left\{\frac{\omega L}{v_o}-\frac{i\omega_p}{2\omega}\left(\frac{\omega-\omega_p}{\omega+\omega_p}\left[\exp\left(iL\,\frac{\omega+\omega_p}{v_o}\right)-1\right]\right.\right.$$
$$\left.\left.-\frac{\omega+\omega_p}{\omega-\omega_p}\left[\exp\left(iL\,\frac{\omega-\omega_p}{v_o}\right)-1\right]\right)\right\}=0 \qquad (1)$$

The assumed variation $e^{-i\omega t}$ implies that when the dominant eigenfrequency recovered (i.e., the one with the uppermost imaginary part) has Im $\omega < 0$, then the classical Pierce diode is stable to linear perturbations; conversely, a dominant eigenfrequency with Im $\omega > 0$ indicates linear instability.

For any axially bounded plasma system, the linear dynamics depend on (i) the plasma equilibrium parameters, (ii) the particle boundary conditions, and (iii) the external circuit (fields) requirements[5]. However, because of its simplicity, the "classical" Pierce diode's linear stability can conveniently be parametrized with the single quantity

$$\alpha = \omega_p L/v_o \qquad (2)$$

where L/v_o is the electron transit time in the unperturbed state. In one customary physical interpretation of α, the values for L and v_o are imagined to be fixed so that any variation in α implies variation in the injected electron current at the cathode.

$$\frac{\omega+\omega_p}{\omega-\omega_p}\frac{\omega}{\omega_p}\left\{\frac{\omega L}{v_o}-\frac{i\omega_p}{2\omega}\left(\frac{\omega-\omega_p}{\omega+\omega_p}\left[\exp\left(iL\,\frac{\omega+\omega_p}{v_o}\right)-1\right]\right.\right.$$
$$\left.\left.-\frac{\omega+\omega_p}{\omega-\omega_p}\left[\exp\left(iL\,\frac{\omega-\omega_p}{v_o}\right)-1\right]\right)\right\}=0 \qquad (1)$$

The assumed variation $e^{-i\omega t}$ implies that when the dominant eigenfrequency recovered (i.e., the one with the uppermost imaginary part) has Im $\omega < 0$, then the classical Pierce diode is stable to linear perturbations; conversely, a dominant eigenfrequency with Im $\omega > 0$ indicates linear instability.

For any axially bounded plasma system, the linear dynamics depend on (i) the plasma equilibrium parameters, (ii) the particle boundary conditions, and (iii) the external circuit (fields) requirements[5]. However, because of its simplicity, the "classical" Pierce diode's linear stability can conveniently be parametrized with the single quantity

$$\alpha = \omega_p L/v_o \qquad (2)$$

where L/v_o is the electron transit time in the unperturbed state. In one customary physical interpretation of α, the values for L and v_o are imagined to be fixed so that any variation in α implies variation in the injected electron current at the cathode.

The Pierce diode characteristic relation (1) is transcendental and thus yields infinitely many complex eigenfrequencies, each having a corresponding eigenmode profile for the internal electrostatic field E(x) or potential $\phi(x)$. The imaginary parts of this set of eigenfrequencies are bounded from above i.e., there is always an uppermost or "dominant" eigenfrequency ω_1 corresponding to a rate of maximum growth or least damping; the eigenfrequency with the next lower imaginary part will be called the "next-to-dominant". In his first analysis[1], Pierce could examine only the transition to instabilit as α increased through the first threshold at $\alpha = \pi$ (so that the imaginary part of the dominant eigenfrequency passed from negative to positive). Frey and Birdsall[2] calculated the imaginary part of the eigenfrequencies. Recently, more detailed linear analyses of the Pierce diode have numerically evaluated the set of top eigenfrequencies[3-5] and the corresponding eigenmode profiles[5] of E(x) and $\phi(x)$. The top few complex eigenfrequencies returned from the above characteristic equation are shown plotted against α in Fig. 1. It is these top few eigenfrequencies that should normally dominate the Pierce diode small amplitude perturbation behavior. From Fig. 1 it is clear that as a function of α, the system's perturbation behavior is in fact divided into discrete regimes delimited by integer-π increments.

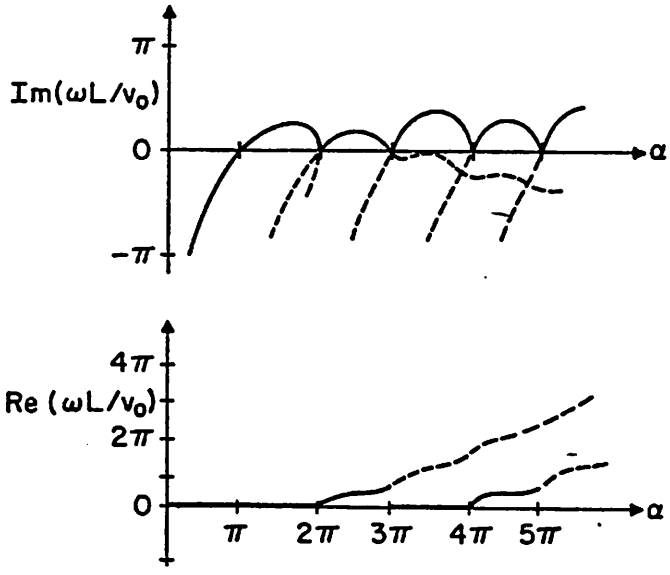

Figure 1. Complex dominant eigenfrequencies (solid curves) of the Pierce diode linear characteristic equation (1) as a function of the single free parameter $\alpha = \omega_p L/v_o$. Frequencies are normalized as indicated, to the transit frequency.
(a) $\mathrm{Im}(\omega L/v_o)$, (b) $\mathrm{Re}(\omega L/v_o)$. (After Godfrey[4])

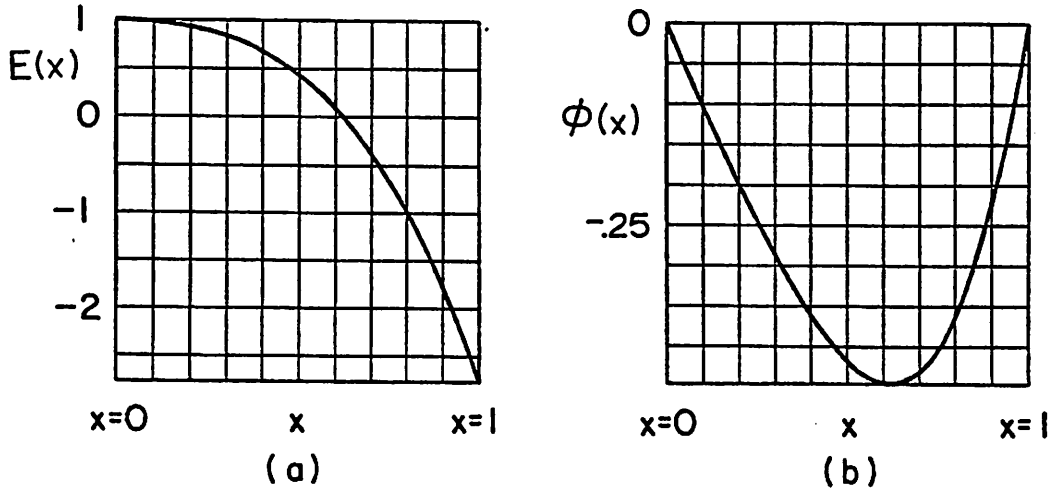

Figure 2. Calculated theoretical profiles of the dominant linear eigenmode for the case $\alpha = 0.5\pi$. (a) Electric field E(x), (b) potential $\phi(x)$.

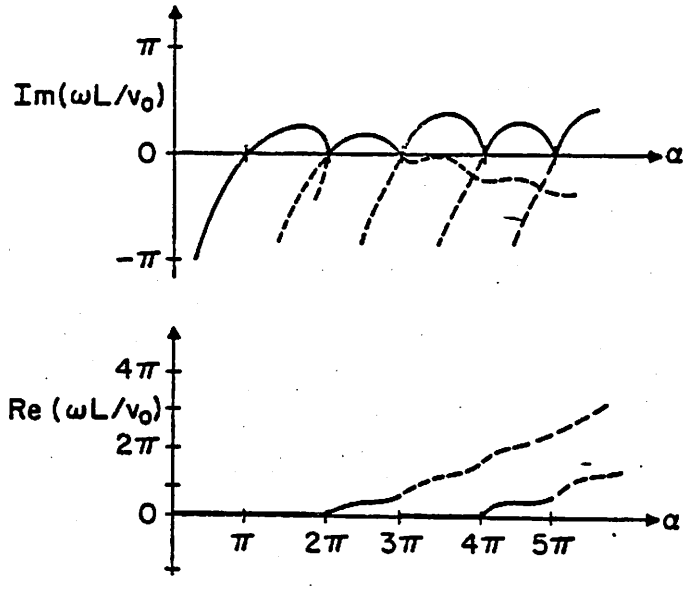

Figure 1. Complex dominant eigenfrequencies (solid curves) of the Pierce diode linear characteristic equation (1) as a function of the single free parameter $\alpha = \omega_p L/v_o$. Frequencies are normalized as indicated, to the transit frequency. (a) $\mathrm{Im}(\omega L/v_o)$, (b) $\mathrm{Re}(\omega L/v_o)$. (After Godfrey[4])

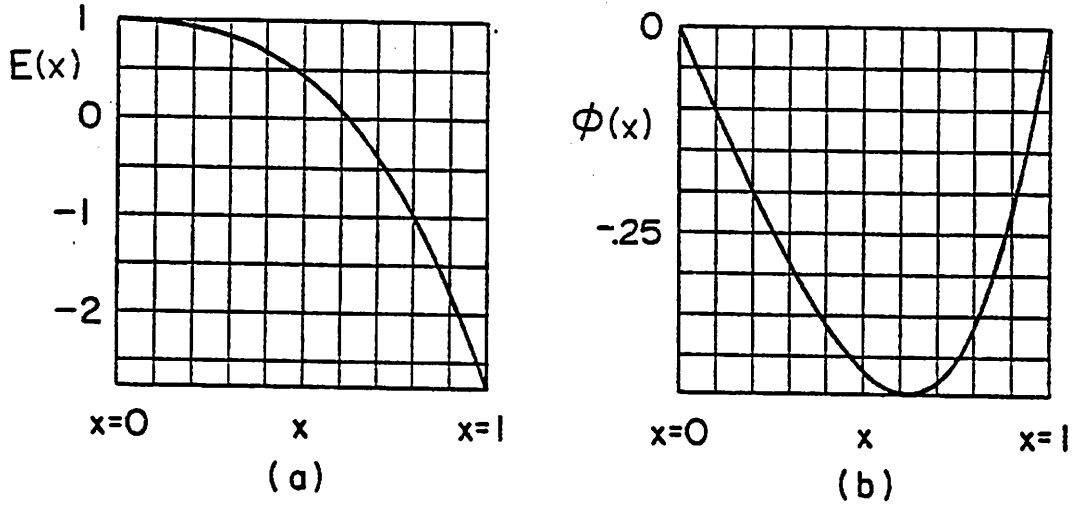

Figure 2. Calculated theoretical profiles of the dominant linear eigenmode for the case $\alpha = 0.5\pi$. (a) Electric field E(x), (b) potential $\phi(x)$.

In one recent paper,[5] the Pierce diode linear response to an arbitrary, small, initial perturbation is predicted to have well defined characteristics, divided into several stages. Looking first at the internal behavior, the electrostatic fields should experince three stages of linear response. During the first, or "initial transit" stage, $0 < t < L/v_o$, the perturbed field profile should show a generally complex pattern that exhibits oscillations at both the plasma frequency and the eigenfrequencies, and exits the system along with the original electrons. What is left behind is a pure collection of eigenmodes; the respective amplitudes of these depend directly on the details of the initial perturbation. The second, or "adjustment" stage is some period beyond time $t = L/v_o$ during which these independent eigenmodes grow and decay competitively at their respective eigenfrequencies. In many cases of interest, there is a third, or "dominant eigenmode" stage in the linear response, in which all eigenmodes except the dominant are negligible. While all three of these stages are in fact linear, the "dominant eigenmode" stage is what is usually referred to loosely as "the linear stage" of the system's perturbation response. The initial transient (first and second) stages are a quite complex process, perhaps deserving more exact study than we provide here; our primary interest in this paper is in the dominant eigenmode (linear) and final (non-

linear) stages. The external perturbation response of the Pierce diode is the perturbed external current, $J_{ext}(t) - J_o$. In contrast to the internal response, the external current should be[5] only a superposition of eigenfrequency oscillations (i.e., it should exhibit no plasma frequency oscillations even during the "initial transit" stage).

Only the first three α regimes ($\alpha = 0$ to π , π to 2π , 2π to 3π) are considered in this paper, and results for these will be reported in separate sections below. Within these first three α regimes, all four possible types of dominant linear eigenfrequencies $\omega_1 = \omega_{1r} + i\gamma_1$ are evidenced: Within the first regime $0 < \alpha < \pi$, there is pure damping and the diode is stable: $\omega_{1r} = 0$, $\gamma_1 < 0$. Within the second regime $\pi < \alpha < 2\pi$, the diode is unstabe showing "pure growth": $\omega_{1r} = 0$, $\gamma_1 > 0$. The third regime has two subdivisions. For most of this regime $2\pi < \alpha < 3\pi - \epsilon$ where $\epsilon \ll \pi$, oscillations with growth are found: $\omega_{1r} \neq 0$, $\gamma_1 > 0$. In the remainder of the third regime $2\pi - \epsilon < \alpha < 3\pi$, damped oscillations are found: $\omega_{1r} \neq 0$, $\gamma_1 < 0$; simulations of this regime and higher α-regimes will be left for the future. Above $\alpha = 3\pi$, the pattern of the second and third regimes basically repeats; as α is increased, the dominant growth rates γ_1 / ω_{1r} decrease, and while it may not be obvious from Fig. 1, the Pierce diode in the limit $L \to \infty$ is again stable, having $\gamma_1 \to 0$.

linear) stages. The external perturbation response of the Pierce diode is the perturbed external current, $J_{ext}(t) - J_o$. In contrast to the internal response, the external current should be[5] only a superposition of eigenfrequency oscillations (i.e., it should exhibit no plasma frequency oscillations even during the "initial transit" stage).

Only the first three α regimes ($\alpha = 0$ to π , π to 2π , 2π to 3π) are considered in this paper, and results for these will be reported in separate sections below. Within these first three α regimes, all four possible types of dominant linear eigenfrequencies $\omega_1 = \omega_{1r} + i\gamma_1$ are evidenced: Within the first regime $0 < \alpha < \pi$, there is pure damping and the diode is stable: $\omega_{1r} = 0$, $\gamma_1 < 0$. Within the second regime $\pi < \alpha < 2\pi$, the diode is unstabe showing "pure growth": $\omega_{1r} = 0$, $\gamma_1 > 0$. The third regime has two subdivisions. For most of this regime $2\pi < \alpha < 3\pi - \epsilon$ where $\epsilon \ll \pi$, oscillations with growth are found: $\omega_{1r} \neq 0$, $\gamma_1 > 0$. In the remainder of the third regime $2\pi - \epsilon < \alpha < 3\pi$, damped oscillations are found: $\omega_{1r} \neq 0$, $\gamma_1 < 0$; simulations of this regime and higher α-regimes will be left for the future. Above $\alpha = 3\pi$, the pattern of the second and third regimes basically repeats; as α is increased, the dominant growth rates γ_1 / ω_{1r} decrease, and while it may not be obvious from Fig. 1, the Pierce diode in the limit $L \to \infty$ is again stable, having $\gamma_1 \to 0$.

The simulations that are presented in this paper were done using the new particle code PDW1.[6] This PIC code was developed to handle general 1-d,(1,2,3)-v electrostatic axially bounded plasma problems, i.e., is not specialized to just the Pierce diode. For reference, all runs discussed in this report were standardized to involve some 2000 simulation particles (the precise number varies during each run). Fields are calculated on a grid of 128 points using a finite-difference Poisson scheme (i.e., not using Fourier-transformed fields and thus without any smooting in k-space). During the simulations, the imposed boundary conditions ensure first that electrons are injected at a constant rate from the cathode ($x = 0$), and second, that any of these electrons reaching either electrode are absorbed, contributing either to the surface charge or to the external circuit current, according to the requirements of the external short circuit. All runs were initialized by prescribing electron spatial distributions which differ only slightly from the uniform classical equilibrium. When this equilibrium is stable, our simulations recover the predicted linear behavior, the perturbations decaying back to the uniform equilibrium. When it is unstable, these simulations proceed beyond the linear regime to recover the subsequent nonlinear behavior as well.

II. FIRST REGIME: $0 < \alpha < \pi$

Analysis:

In the first α-regime, the Pierce diode characteristic equation (1) returns a dominant linear eigenfrequency that is negative imaginary, $\omega_1 = i\gamma_1$ with $\gamma_1 < 0$, and the diode in this α-regime is said to be stable. The lower eigenmodes are oscillatory ($\mathrm{Re}\,\omega \neq 0$) but they are all decaying ($\mathrm{Im}\,\omega < 0$) even faster than the dominant[5].

For a representative value in this regime of $\alpha = 0.5\pi$, the dominant eigenfrequency has been calculated[5] from (1) and is $\omega_1 / \omega_p = -1.227i$. The corresponding perturbation eigenmode profiles have also been calculated theoretically[5] and are shown in Fig. 2. Here and for all subsequent theoretical eigenmode profiles shown, E(x) is normalized such that $E(x=0) = 1$ and $\phi(x) = -\int_0^x E(s)ds$. For convencience, x will always be plotted in units normalized to L, i.e., $L \to 1$. Note first that $|\phi|_{max}$ is located off center at x = 0.62, i.e., closer to the anode than to the electron injection plane; also, the end values of E(x) differ in sign and magnitude. This, of course, means that the total charge of the plasma region is nonzero, and that the surface charges on the two end plates are different. For future reference, the next-to-dominant eigenfrequency is fully complex with theoretical value $\omega_2 / \omega_p = 5.412 - 2.546i$.

II. FIRST REGIME: $0 < \alpha < \pi$

Analysis:

In the first α-regime, the Pierce diode characteristic equation (1) returns a dominant linear eigenfrequency that is negative imaginary, $\omega_1 = i\gamma_1$ with $\gamma_1 < 0$, and the diode in this α-regime is said to be stable. The lower eigenmodes are oscillatory ($\mathrm{Re}\,\omega \neq 0$) but they are all decaying ($\mathrm{Im}\,\omega < 0$) even faster than the dominant[5].

For a representative value in this regime of $\alpha = 0.5\pi$, the dominant eigenfrequency has been calculated[5] from (1) and is $\omega_1 / \omega_p = -1.227i$. The corresponding perturbation eigenmode profiles have also been calculated theoretically[5] and are shown in Fig. 2. Here and for all subsequent theoretical eigenmode profiles shown, E(x) is normalized such that $E(x=0) = 1$ and $\phi(x) = -\int_0^x E(s)ds$. For convencience, x will always be plotted in units normalized to L, i.e., $L \to 1$. Note first that $|\phi|_{max}$ is located off center at x = 0.62, i.e., closer to the anode than to the electron injection plane; also, the end values of E(x) differ in sign and magnitude. This, of course, means that the total charge of the plasma region is nonzero, and that the surface charges on the two end plates are different. For future reference, the next-to-dominant eigenfrequency is fully complex with theoretical value $\omega_2 / \omega_p = 5.412 - 2.546i$.

Simulations:

The initialzation used for the first simulation runs is shown in Fig. 3. Electron phase space (a scatter-plot of the electron velocities versus position in the diode) is shown in Fig. 3(a) with velocity normalized to v_o i.e., $v_o \rightarrow 1$. The normalization choices $L = 1$ and $v_o = 1$ imply that time is effectively measured in electron transit periods; as described earlier, by varying α (in different runs) we are in fact varying the injected electron beam density and thus current: $J_o = -en_o v_o \equiv -\epsilon_o (m/e)(v_o^3/L^2)\alpha^2$. Further simplification is possible by specifying physical units $e/m = 1$ and $\epsilon_o = 1$ such that $\omega_p = \alpha$ and $J_o = -\alpha^2$.

The initial perturbation in charge density $\rho(x;t=0)$ is given a sinusoidal shape as shown in Fig. 3(b), achieved by spacing the loaded electrons near the ends of the diode more closely together than those in the center. By choice, the total number of simulation electrons in the initialization is such as to ensure overall neutrality for the plasma region. The plasma system's total active charge (i.e., excluding charges on the walls) is defined as

$$Q_{active}(t) \equiv \int_0^L \rho(x,t)dx = \epsilon_o \left[E(x=L,t)-E(x=0,t)\right] . \qquad (3)$$

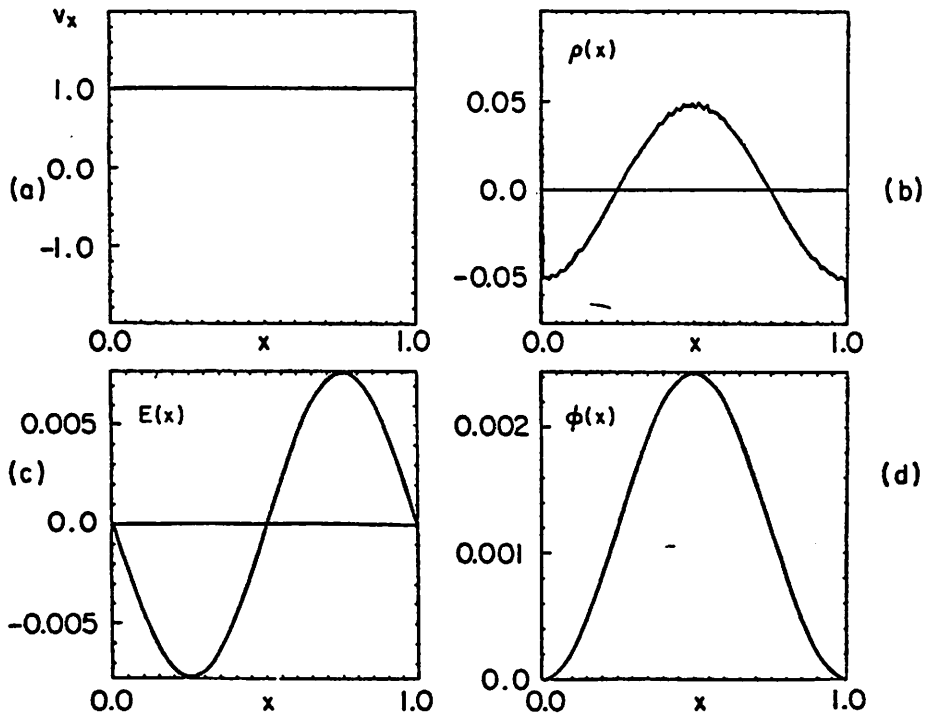

Figure 3. Initial conditions used in Pierce diode simulations for the case $\alpha = 0.5\pi$. (a) Electron phase space v versus x, (b) Charge density $\rho(x) = e(n_o - n_e(x))$, (c) resulting electric field E(x), and (d) potential profile $\phi(x) > 0$, indicating "positive initialization".

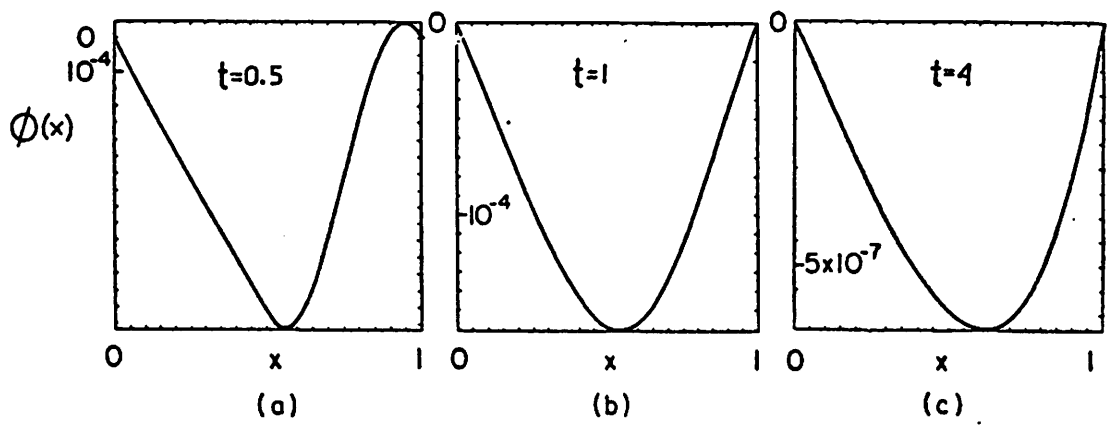

Figure 4. Case: $\alpha = 0.5\pi$, positive initialization. Potential profiles $\phi(x)$ at times t = 0.5, 1, and 4. Note that the ordinate on each plot is scaled according to the respective maximum values of ϕ.

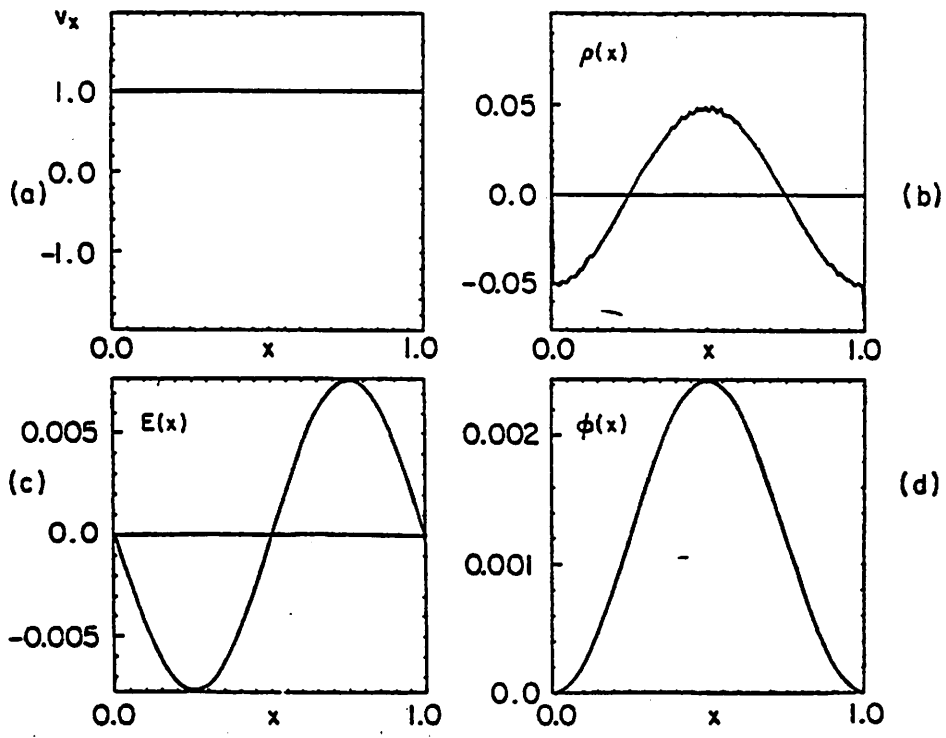

Figure 3. Initial conditions used in Pierce diode simulations for the case $\alpha = 0.5\pi$. (a) Electron phase space v versus x, (b) Charge density $\rho(x) = e(n_o - n_e(x))$, (c) resulting electric field E(x), and (d) potential profile $\phi(x) > 0$, indicating "positive initialization".

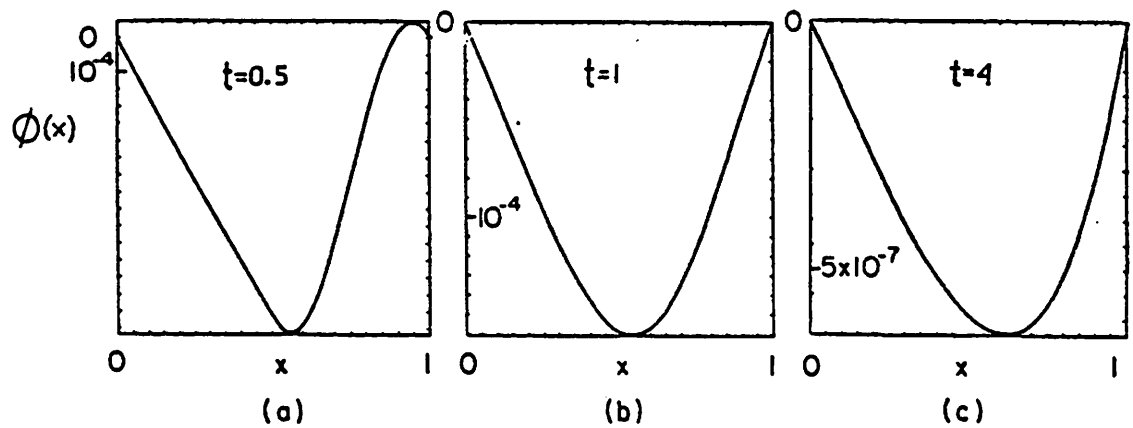

Figure 4. Case: $\alpha = 0.5\pi$, positive initialization. Potential profiles $\phi(x)$ at times t = 0.5, 1, and 4. Note that the ordinate on each plot is scaled according to the respective maximum values of ϕ.

Overall neutrality of the diode region is equivalent to having $E(x=0) = E(x=L)$, as has been chosen for the initialization here, shown in Fig. 3(b) and (c).

The corresponding initial potential profile $\phi(x)$ shown in Fig. 3(d) is everywhere positive. For all runs in this paper, the initial perturbation potential energy in the system is less than 0.1% of the total particle kinetic energy. Values indicated for the plotted simulation potentials are normalized to $\phi_o = mv_o^2/e$, i.e., differ from the normalization used for the earlier plots of theoretical potential eigenmodes in Fig. 2.

It would also have been easy to space the initial electrons closer together towards the diode center, in which case the resulting initialization profiles $\rho(x)$, $E(x)$, and $\phi(x)$ would all have had just the opposite signs from those shown in Fig. 3. For ease of reference, these two overall neutral initializations with sinusoidal potential profiles of opposite signs will hereafter be called "positive" or "negative"; keep in mind however that both are in fact overall neutral. A non-neutral initialzation scheme would have served as well as this neutral one.

Snapshots of the potential profile at three times are shown in Fig. 4. Note that the sign of the potential profile reverses within the first electron transit time: as the initialized electrons exit the diode, the associated oscillating profile $\phi(x,t)$ leaves with them, Fig. 4(a), followed by the

newly injected electrons which fill the diode form the left and uncover the expected set of linear eigenmodes. The initial $\phi(x)$ profile does not really evolve into the dominant linear eigenmode, rather a complex pattern associated with the initial perturbation transits the system, in agreement with the earlier description of the expected[5] first stage of the system's response.

Once the initial electrons and associated potential profile have completely transited the diode, the potential profile remaining, Fig. 4(b), clearly differs from the dominant eigenmode shape, Fig. 2(b). In this "adjustment" stage, the lower eigenmodes present are still significant, but as these decay (relative to the dominant) the profile evolves into the dominant shape alone.

The dominant eigenmode stage is exemplified by the potential profile of Fig. 4(c), showing no significant contamination when compared with Fig. 2(b). (The agreement in sign between the calculated profile in Fig. 2 and the simulation profiles in Fig. 4 results simply from the choice of "positive" initialization for the simulation; when the diode is initialized "negatively", the recovered simulation potential profiles have signs opposite to that shown here.) In

newly injected electrons which fill the diode form the left and uncover the expected set of linear eigenmodes. The initial $\phi(x)$ profile does not really evolve into the dominant linear eigenmode, rather a complex pattern associated with the initial perturbation transits the system, in agreement with the earlier description of the expected[5] first stage of the system's response.

Once the initial electrons and associated potential profile have completely transited the diode, the potential profile remaining, Fig. 4(b), clearly differs from the dominant eigenmode shape, Fig. 2(b). In this "adjustment" stage, the lower eigenmodes present are still significant, but as these decay (relative to the dominant) the profile evolves into the dominant shape alone.

The dominant eigenmode stage is exemplified by the potential profile of Fig. 4(c), showing no significant contamination when compared with Fig. 2(b). (The agreement in sign between the calculated profile in Fig. 2 and the simulation profiles in Fig. 4 results simply from the choice of "positive" initialization for the simulation; when the diode is initialized "negatively", the recovered simulation potential profiles have signs opposite to that shown here.) In

this stable α-regime, the dominant eigenmode stage is the final stage of the Pierce diode's perturbation response: the potential profile is seen to retain this dominant eigenmode shape while its amplitude gets progressively smaller. The recovered electric field profiles E(x) (not shown) evolve correspondingly into the correct eigenmode shape, and from the boundary values (see Fig. 2(a)) it is clear that in this stage the diode has a net negative overall active charge: $Q_{active}(t)$ approaches zero from the negative side.

As a global measure of the system's evolution it proves convenient to define an "internal electrostatic energy" at any instant as

$$W_i(t) = \frac{1}{2} \int_0^L \rho(x,t)\phi(x,t)dx. \qquad (4)$$

The temporal behavior of $W_i(t)$ plotted in Fig. 5(a) is taken from the simulation for $\alpha = 0.5\pi$. While at first ($t \lesssim 3.5$) there are apparently some transients correlated with the "initial-transit" and "adjustment" stages, ultimately $W_i(t)$ shows simple exponential decay. We also define an instaneous rate of change

$$\gamma_W(t) = \frac{d}{dt} \ln W_i(t) \qquad (5)$$

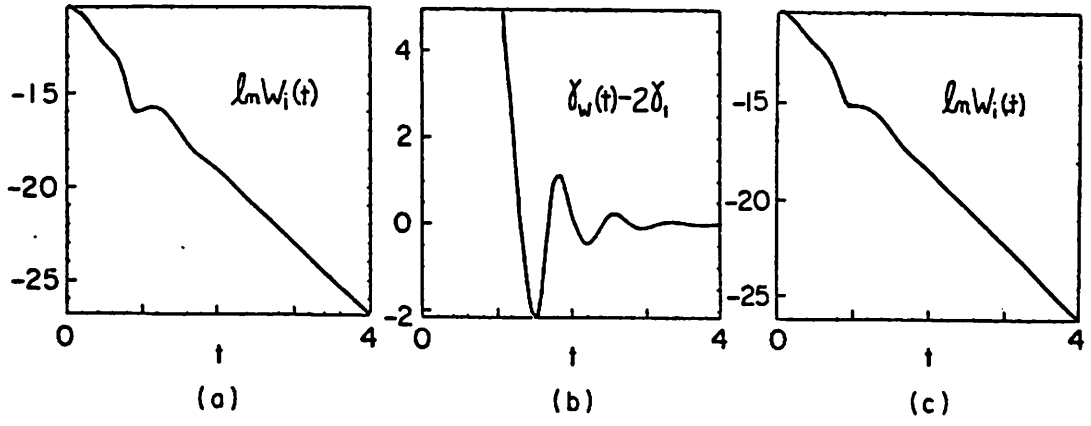

Figure 5. Case: $\alpha = 0.5\pi$, positive initialization. (a) Internal electrostatic energy plot, $\ln W_1(t)$, (b) the difference between the simulation energy rate of change, $\gamma_W(t)$, and the expected decay rate for the dominant-eigenmode change, $2\gamma_1$ (not evaluated for $t < 1$ to avoid "initial transit" stage), and (c) history plot of of $\ln W_1(t)$ for the diode initialized with negative potential $\phi(x)$.

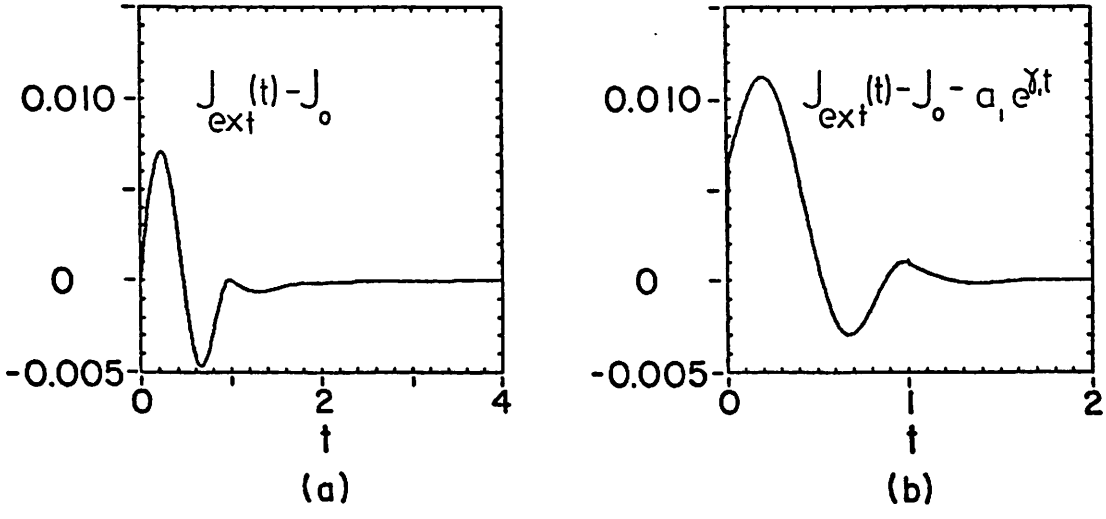

Figure 6. Case: $\alpha = 1.5\pi$, positive initialization. (a) Perturbation external current, $J_{ext}(t)-J_o$, for $t < 4$, (b) External current minus the dominant-eigenmode contribution, $J_{ext}(t) - J_o - a_1\exp(\gamma_1 t)$, from which the next-to-dominant eigenfrequency is directly recovered.

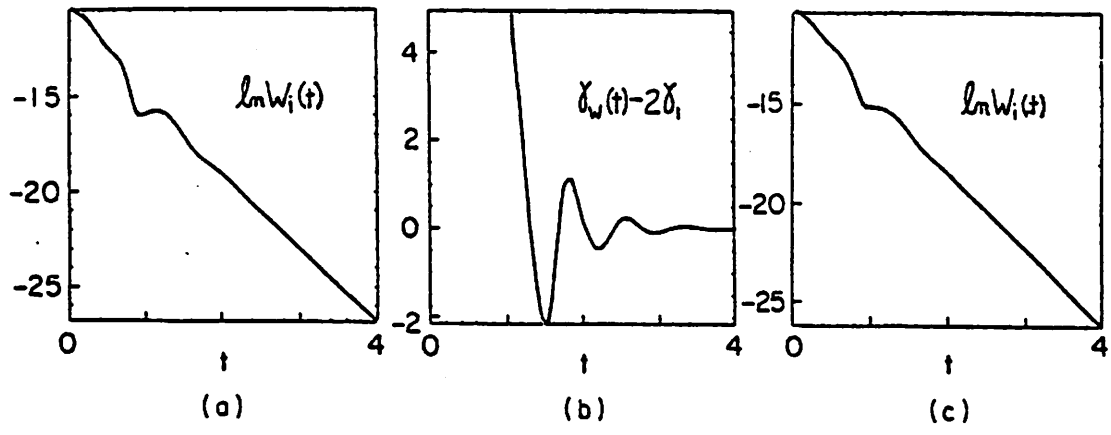

Figure 5. Case: $\alpha = 0.5\pi$, positive initialization. (a) Internal electrostatic energy plot, $\ln W_i(t)$, (b) the difference between the simulation energy rate of change, $\gamma_w(t)$, and the expected decay rate for the dominant-eigenmode change, $2\gamma_1$ (not evaluated for $t < 1$ to avoid "initial transit" stage), and (c) history plot of of $\ln W_i(t)$ for the diode initialized with negative potential $\phi(x)$.

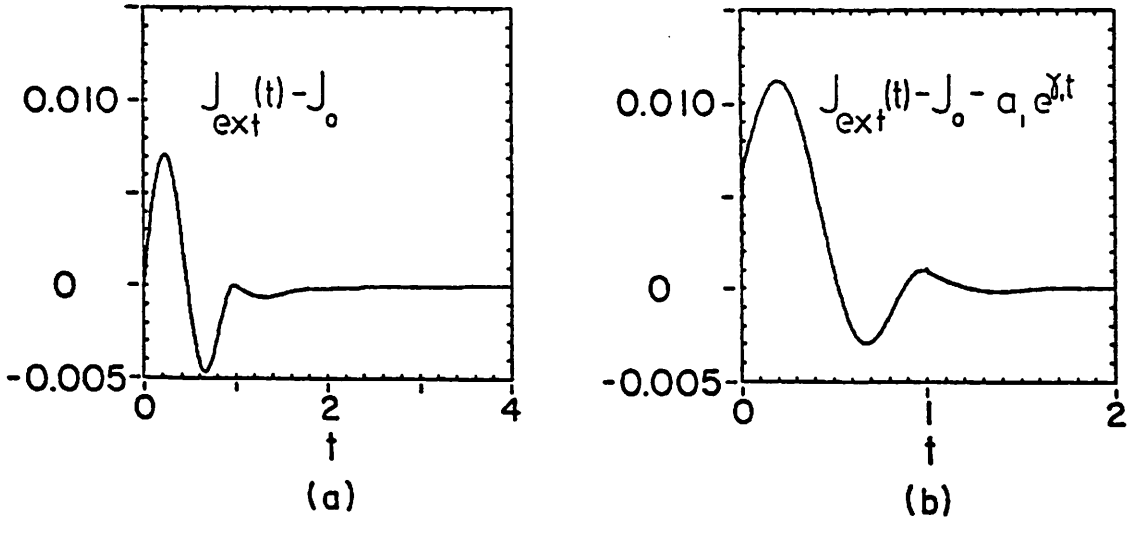

Figure 6. Case: $\alpha = 1.5\pi$, positive initialization. (a) Perturbation external current, $J_{ext}(t)-J_o$, for $t < 4$, (b) External current minus the dominant-eigenmode contribution, $J_{ext}(t) - J_o - a_1\exp(\gamma_1 t)$, from which the next-to-dominant eigenfrequency is directly recovered.

which will prove convenient in comparing simulation results with the oscillation frequencies, growth and damping rates predicted theoretically for the eigenmodes.

In the present case of $\alpha = 0.5\pi$, where the dominant eigenmode is purely decaying, we expect that in the dominant-eigenmode stage γ_W becomes constant and equal to $2\gamma_1$. The difference $\gamma_W(t) - 2\gamma_1$ is plotted in Fig. 5(b). From this figure, note first that the simulation decay rate, $\gamma_W(t)$, does eventually approach the expected linear value $2\gamma_1$ as the simulation diode progresses towards its final "dominant eigenmode" stage; then note that before the final stage is reached, $\gamma_W(t)$ oscillates around its final value, $2\gamma_1$. Having in this sense subtracted out the dominant eigenfrequency from $W_i(t)$, then the remaining quite regular oscillation frequency can be obtained by simply measuring the distance between zero crossings. The oscillation frequency recovered this way shows $\omega/\omega_p = 5.4$, in good agreement with the real part of the theoretical next-to-dominant eigenfrequency given earlier. The reasonable inference is thus that this observed oscillation in the internal electrostatic energy (in the period $1 < t \lesssim 3.5$) corresponds to the second linear stage discussed above, when the diode system should contain a collection of eigenmodes, all other eigenmodes decaying even faster than the dominant one.

Inside the diode there are particle and displacement currents, both of which can vary with location in the diode; but in a 1-d system, their total must at every instant equal the external (conduction) current. Thus as a last Pierce diode simulation diagnostic, it is convenient and helpful to monitor the external current history $J_{ext}(t)$. It can be shown that whenever $Q_{active} = 0$, then $J_{ext}(t) = J_o$. As a consequence, the initialization in Fig. 3 implies that $J_{ext}(t=0) = J_o$.

The subsequent perturbation current $J_{ext}(t) - J_o$ for $\alpha = 0.5\pi$ is shown in Fig. 6(a). In this stable α-regime, this external current perturbation is always a linear sum of eigenmodes. As already mentioned, this external diagnostic is also predicted[5] to contain no plasma frequency oscillations, unlike the internal response. In being linear, it also differs from the above internal total electrostatic energy diagnostic $\gamma_W(t)$, which involves the logarithm of a quadratic quantitiy. Thus in the dominant eigenmode stage ($t \gtrsim 3.5$ in this case) the external current perturbation should be readily resolvable, not only in frequency, ω_1, but also in amplitude, a_1. For this measurement, we have used the simple single-frequency, four-point alogrithm given in Ref. 12.

It is then possible, as shown in Fig. 6(b) for $t < 2$, to subtract off completely the dominant eigenmode $a_1 e^{-i\omega_1 t}$,

Inside the diode there are particle and displacement currents, both of which can vary with location in the diode; but in a 1-d system, their total must at every instant equal the external (conduction) current. Thus as a last Pierce diode simulation diagnostic, it is convenient and helpful to monitor the external current history $J_{ext}(t)$. It can be shown that whenever $Q_{active} = 0$, then $J_{ext}(t) = J_o$. As a consequence, the initialization in Fig. 3 implies that $J_{ext}(t=0) = J_o$.

The subsequent perturbation current $J_{ext}(t) - J_o$ for $\alpha = 0.5\pi$ is shown in Fig. 6(a). In this stable α-regime, this external current perturbation is always a linear sum of eigenmodes. As already mentioned, this external diagnostic is also predicted[5] to contain no plasma frequency oscillations, unlike the internal response. In being linear, it also differs from the above internal total electrostatic energy diagnostic $\gamma_W(t)$, which involves the logarithm of a quadratic quantitiy. Thus in the dominant eigenmode stage ($t \gtrsim 3.5$ in this case) the external current perturbation should be readily resolvable, not only in frequency, ω_1, but also in amplitude, a_1. For this measurement, we have used the simple single-frequency, four-point alogrithm given in Ref. 12.

It is then possible, as shown in Fig. 6(b) for $t < 2$, to subtract off completely the dominant eigenmode $a_1 e^{-i\omega_1 t}$,

from the external perturbation, leaving all the lower eigenmodes. In this case after the next-to-dominant takes over, the simple four-point measure[12] can again be applied to the curve shown in Fig. 6(b), this time yielding a_2 and ω_2; in the present case, we find $\omega_2/\omega_p = 5.56 - 2.53i$, in good agreement with the theoretical prediction given earlier.

In principle, this scheme of subtracting successive eigenmodes to uncover the next-lower ones could be iterated down to the accuracy of the simulation.

Another simulation was run, this time with a negative initial potential profile (electrons initialized slightly towards the center of the diode). The observed simulation "initial-transit" and "adjustment" stages are very similar to those detailed above for the case of positive initial potential profile. And again, in the dominant-eigenmode stage the observed potential and electric field profiles attain their corresponding eigenmode shapes (Fig. 2) but now with signs opposite to those shown above (which involved positive initial potential perturbation); this result is consistent with the linear nature of our problem, in that the eigenmode profiles are determined only to within an arbitrary constant factor. The final decay rate of $W_i(t)$ is found to have the same value as before, $2\gamma_1$. As a consequence of the sign reversals on the field profiles, $Q_{active}(t)$ in the final stage is also reversed and now falls asymptotically to zero from the positive side.

To conclude, when operating the Pierce diode in the first regime, $0 < \alpha < \pi$, the final state found in our simulations of the system is in fact the neutral, classical Pierce equilibrium. This equilibrium is stable. Several features of predicted linear behavior, including the initial transients, and the dominant and next-to-dominant eigenfrequencies have been recovered. The simulation results have been found to depend on the sign of the initialization exactly as expected.

To conclude, when operating the Pierce diode in the first regime, $0 < \alpha < \pi$, the final state found in our simulations of the system is in fact the neutral, classical Pierce equilibrium. This equilibrium is stable. Several features of predicted linear behavior, including the initial transients, and the dominant and next-to-dominant eigenfrequencies have been recovered. The simulation results have been found to depend on the sign of the initialization exactly as expected.

III. SECOND REGIME: $\pi < \alpha < 2\pi$

Analysis:

In the second α-regime, the Pierce characteristic relation (1) again returns a dominant eigenfrequency that is purely imaginary, but now it lies in the upper half-plane, indicating an instability that is sometimes characterized as "purely growing"; all other eigenmodes are decaying. The diode internal linear response to any initial perturbation should again pass first through an initial transit stage ($t \leq 1$) during which the original electrons exit the diode. Next there should be an adjustment stage during which the diode is filled with a pure collection of eigenmodes, of which all but the dominant one are decaying. The dominant eigenmode will quickly emerge from the others, and for some period of time should show linear growth at a rate that corresponds to the dominant eigenfrequency (positive imaginary). Of course in an unstable system the final stage cannot be the initial configuration as happened in the stable $\alpha = 0.5\pi$ case: the perturbation will grow beyond the realm of linear validity, resulting ultimately in a system configuration which differs significantly from the original uniform equilibrium around which our linear analysis was based.

Using the representative value $\alpha = 1.5\pi$, the dominant eigenfrequency calculated[5] from the characteristic equation (1) is $\omega_1/\omega_p = +0.1625i$; for future reference, the next-to-dominant eigenfrequency is fully complex with value $\omega_2/\omega_p = 2.5180 - 0.6869i$. The corresponding theoretical dominant-eigenmode profiles are shown in Fig. 7 and are seen to differ significantly from the ones calculated earlier for $\alpha = 0.5\pi$ (Fig. 2). For example, the potential profile now has its extremum closer to the electron injection plane than to the anode, at x = 0.37.

Simulations:

Again a small initial perturbation is imposed upon the uniform classical Pierce equilibrium by bunching the electrons slightly at each end to ensure that the initial potential profile is everywhere positive (i.e., the initial conditions are again as shown in Fig. 3).

Snapshots of the simulation potential profiles and the corresponding phase-space plots are shown in Figs. 8(a) and (b), respectively. Already at t = 1.5, i.e., soon after the initial-transit stage, the potential profile is seen to have adjusted into a shape very close to the calculated eigenmode's (shown in Fig. 7(b)). Unlike the $\alpha = 0.5\pi$ case, the sign of the potential $\phi(x)$ now happens to be the same as the initial condition's. The amplitude of this profile is seen to

Using the representative value $\alpha = 1.5\pi$, the dominant eigenfrequency calculated[5] from the characteristic equation (1) is $\omega_1/\omega_p = +0.1625i$; for future reference, the next-to-dominant eigenfrequency is fully complex with value $\omega_2/\omega_p = 2.5180 - 0.6869i$. The corresponding theoretical dominant-eigenmode profiles are shown in Fig. 7 and are seen to differ significantly from the ones calculated earlier for $\alpha = 0.5\pi$ (Fig. 2). For example, the potential profile now has its extremum closer to the electron injection plane than to the anode, at x = 0.37.

Simulations:

Again a small initial perturbation is imposed upon the uniform classical Pierce equilibrium by bunching the electrons slightly at each end to ensure that the initial potential profile is everywhere positive (i.e., the initial conditions are again as shown in Fig. 3).

Snapshots of the simulation potential profiles and the corresponding phase-space plots are shown in Figs. 8(a) and (b), respectively. Already at t = 1.5, i.e., soon after the initial-transit stage, the potential profile is seen to have adjusted into a shape very close to the calculated eigenmode's (shown in Fig. 7(b)). Unlike the $\alpha = 0.5\pi$ case, the sign of the potential $\phi(x)$ now happens to be the same as the initial condition's. The amplitude of this profile is seen to

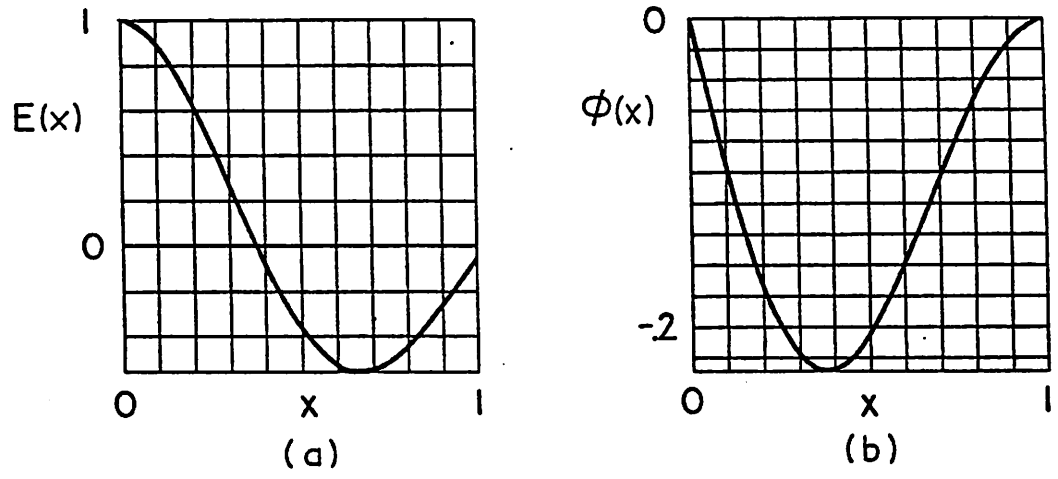

Figure 7. Case: $\alpha = 1.5\pi$. Calculated theoretical dominant eigenmode profiles $E(x)$ and $\phi(x)$.

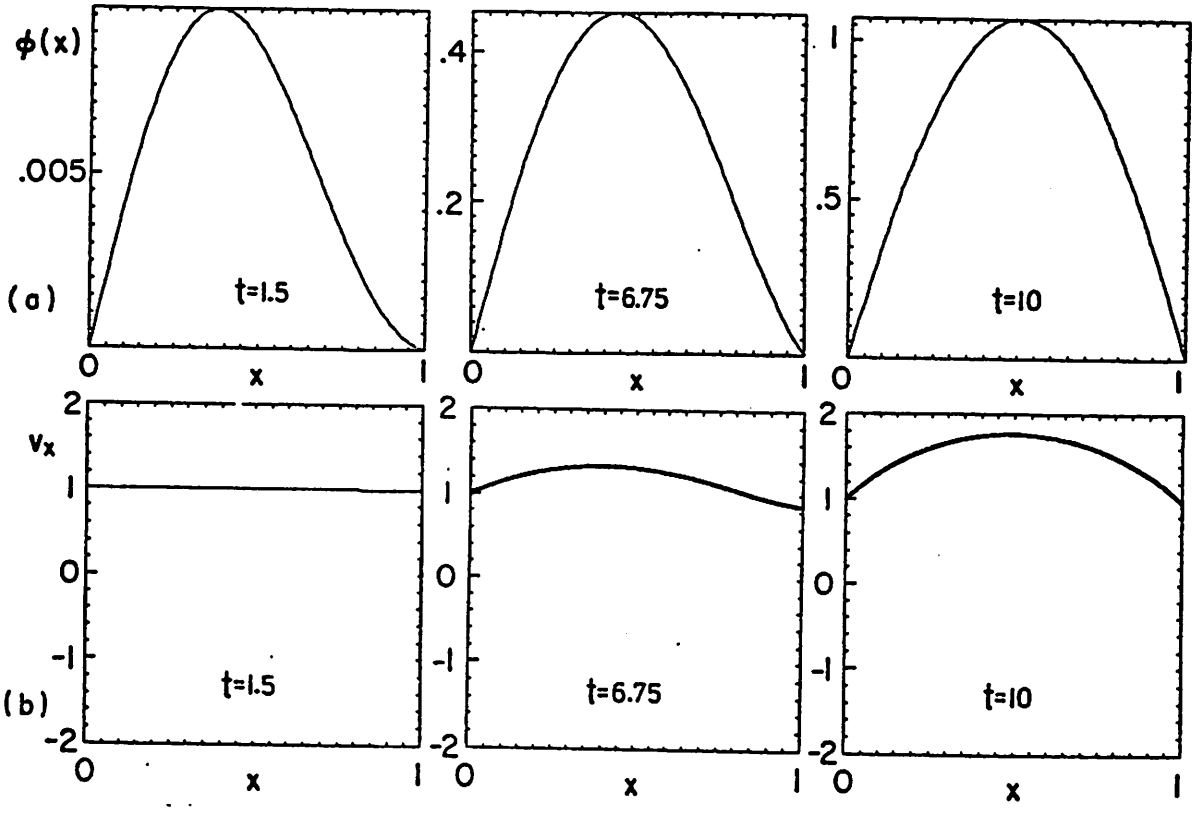

Figure 8. Case: $\alpha = 1.5\pi$, positive initialization. (a) Snapshots of potential profile at t = 1.5, 6.75, and 10, showing linear ("dominant-eigenmode") and nonlinear ("intermediate" and "final saturation") stages, (b) the corresponding electron phase space plots.

be increasing with time. After some period of growth, the $\phi(x)$ profile distorts nonlinearly away from the eigenmode shape, attaining a nearly parabolic form with ϕ_{max} at $x = 0.5$. At the same time, the growth stage evolves into a "saturated" condition and the diode attains a final state which is in fact a new stable equilibrium.

To quantify this growth and saturation, the time behavior of the internal electrostatic energy $W_i(t)$ is plotted in Fig. 9(a). Note first the obvious transients connected with the early initial transit ($0 < t < 1$) and adjustment stages ($1 < t \lesssim 2.5$). Following these transients, the dominant-eigenmode stage is apparent during which $W_i(t)$ shows an almost constant growth rate ($2.5 \lesssim t \lesssim 4$). In the final (saturated) stage, this electrostatic energy growth ceases: $\gamma_W(t) \to 0$.

The plot of $\gamma_W(t) - 2\gamma_1$ (Fig. 9(b)) shows regular oscillations during the adjustment stage, from the peak-times of which the real part of the next-to-dominant eigenfrequency can be fairly well resolved: for this value of $\alpha = 1.5\pi$, the simulation indicates that $\mathrm{Re}(\omega_2)/\omega_p \simeq 2.6$. The transient oscillations are seen to decay as the diode next enters its dominant-eigenmode stage in which $\gamma_W(t)$ approaches the expected[5] value, $2\gamma_1 = 0.325\,\omega_p = +1.53$. What is brought out by Fig. 9(b) (but is not obvious from Fig. 9(a) alone) is that

be increasing with time. After some period of growth, the $\phi(x)$ profile distorts nonlinearly away from the eigenmode shape, attaining a nearly parabolic form with ϕ_{max} at $x = 0.5$. At the same time, the growth stage evolves into a "saturated" condition and the diode attains a final state which is in fact a new stable equilibrium.

To quantify this growth and saturation, the time behavior of the internal electrostatic energy $W_i(t)$ is plotted in Fig. 9(a). Note first the obvious transients connected with the early initial transit ($0 < t < 1$) and adjustment stages ($1 < t \lesssim 2.5$). Following these transients, the dominant-eigenmode stage is apparent during which $W_i(t)$ shows an almost constant growth rate ($2.5 \lesssim t \lesssim 4$). In the final (saturated) stage, this electrostatic energy growth ceases: $\gamma_W(t) \to 0$.

The plot of $\gamma_W(t) - 2\gamma_1$ (Fig. 9(b)) shows regular oscillations during the adjustment stage, from the peak-times of which the real part of the next-to-dominant eigenfrequency can be fairly well resolved: for this value of $\alpha = 1.5\pi$, the simulation indicates that $\mathrm{Re}(\omega_2)/\omega_p \simeq 2.6$. The transient oscillations are seen to decay as the diode next enters its dominant-eigenmode stage in which $\gamma_W(t)$ approaches the expected[5] value, $2\gamma_1 = 0.325\,\omega_p = +1.53$. What is brought out by Fig. 9(b) (but is not obvious from Fig. 9(a) alone) is that

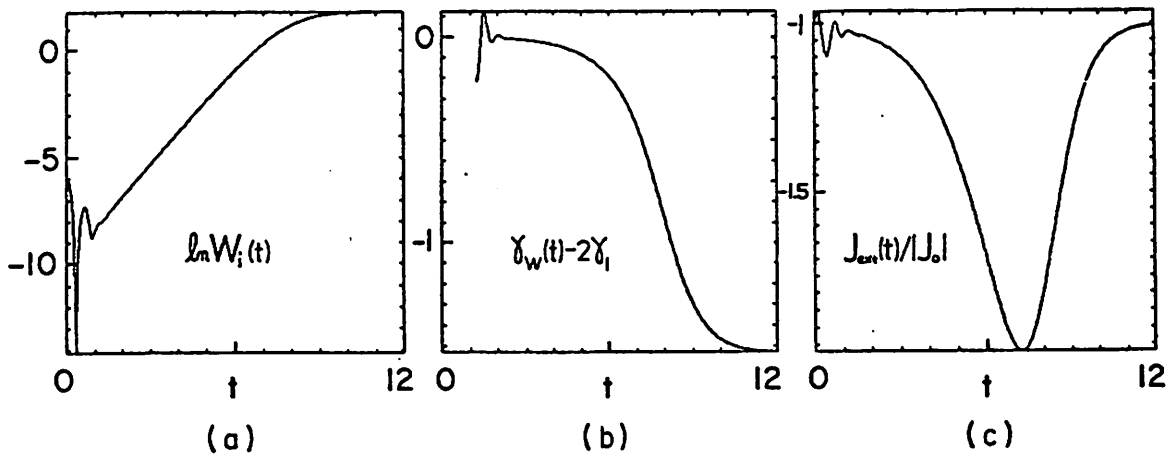

Figure 9. Case: $\alpha = 1.5\pi$, positive initialization. History plots showing (a) the internal electrostatic energy, $\ln W_i(t)$, and (b) the difference between the simulation energy rate of change, $\gamma_W(t)$, and the predicted growth rate in the dominant eigenmode stage, $2\gamma_1$, and (c) the external current, $J_{ext}(t)/|J_o|$.

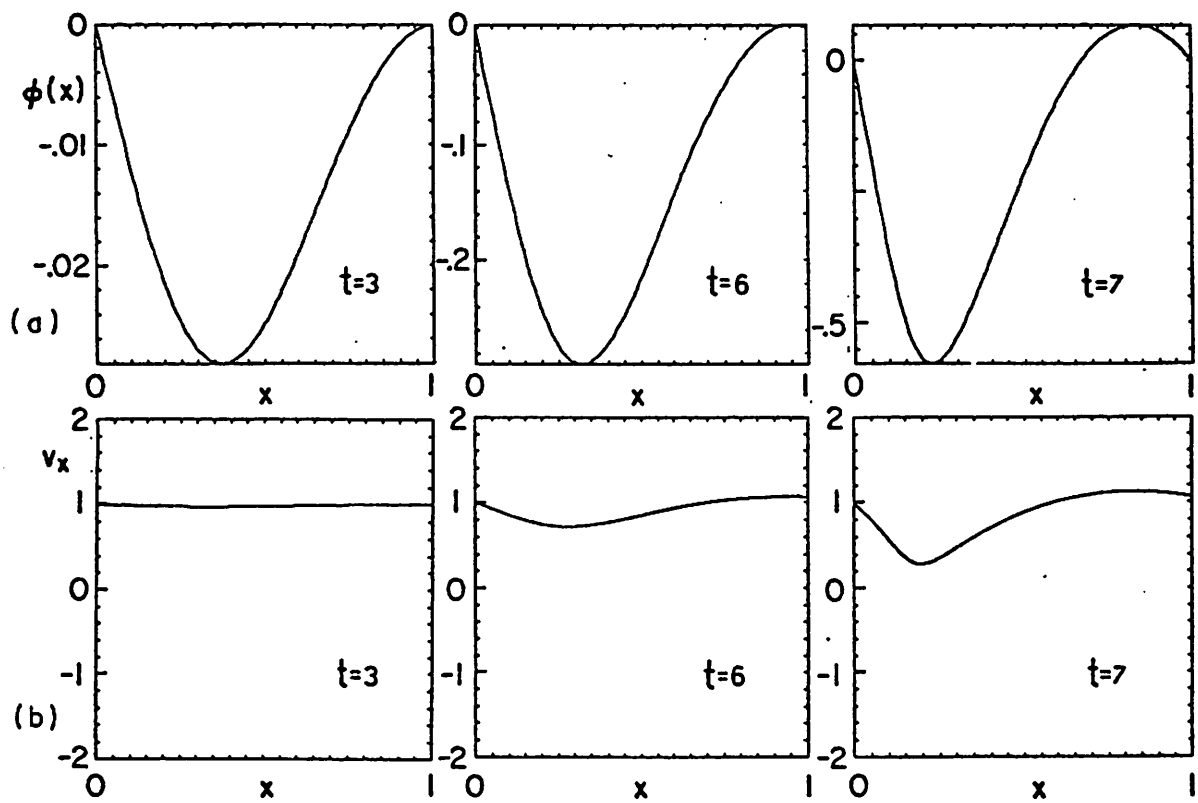

Figure 10. Case: $\alpha = 1.5\pi$, negative initialization. Early behavior of the Pierce diode. Snapshots show diode evolving from linear into nonlinear stages at t = 3, 6, and 7. (a) Potential profiles $\phi(x)$, and (b) the corresponding electron phase spaces.

the nonlinear transition from this dominant-eigenmode stage to the later "saturated" stage is gradual, starting very soon after the adjustment stage transients: the diode exhibits approximately linear behavior for only a limitingly short period of time ($t \lesssim 4$).

The next-to-dominant eigenfrequency is also visible in the external current perturbation $J_{ext}(t)/|J_o|$ for the period $0 < t \lesssim 2$ of Fig. 9(c). Indeed the dominant can be subtracted out and when the observed external oscillations become single-frequency, the simple four-point diagnostic[12] measures the next-to-dominant eigenfrequency to be $\omega_2/\omega_p = 2.5 - 0.55i$. When the next-to-dominant has disappeared, there follows a period of dominant eigenmode growth, during which $J_{ext}(t)$ continuously deforms away from the injection value J_o. Note that $J_{ext}(t)$ first becomes larger (more negative) by nearly a factor of two and in fact shows truly linear behavior only briefly ($2 < t < 4$); as the diode goes nonlinear (i.e., at the same time that $W_i(t)$ is saturating and $\gamma_W(t)$ is going to zero), then it evolves to a new equilibrium in which no electrons are reflected, such that again $J_{ext}(t) = J_o$, the same value as in the original equilibrium.

In the final "saturated" state, the total energy inside the diode (kinetic and electrostatic) is roughly twice what

the nonlinear transition from this dominant-eigenmode stage to the later "saturated" stage is gradual, starting very soon after the adjustment stage transients: the diode exhibits approximately linear behavior for only a limitingly short period of time ($t \lesssim 4$).

The next-to-dominant eigenfrequency is also visible in the external current perturbation $J_{ext}(t)/|J_o|$ for the period $0 < t \lesssim 2$ of Fig. 9(c). Indeed the dominant can be subtracted out and when the observed external oscillations become single-frequency, the simple four-point diagnostic[12] measures the next-to-dominant eigenfrequency to be $\omega_2/\omega_p = 2.5 - 0.55i$. When the next-to-dominant has disappeared, there follows a period of dominant eigenmode growth, during which $J_{ext}(t)$ continuously deforms away from the injection value J_o. Note that $J_{ext}(t)$ first becomes larger (more negative) by nearly a factor of two and in fact shows truly linear behavior only briefly ($2 < t < 4$); as the diode goes nonlinear (i.e., at the same time that $W_i(t)$ is saturating and $\gamma_W(t)$ is going to zero), then it evolves to a new equilibrium in which no electrons are reflected, such that again $J_{ext}(t) = J_o$, the same value as in the original equilibrium.

In the final "saturated" state, the total energy inside the diode (kinetic and electrostatic) is roughly twice what

it was in the initial state (purely kinetic), and is now divided approximately as $W_i \simeq W_{kinetic}/3$. The potential profile $\phi(x)$ is everywhere positive but has a symmetric, nearly parabolic shape, quite different from the dominant eigenmode. Electron phase space indicates that the electrons remain fluid, i.e., that at each x their velocity is single valued. It also shows that the injected electrons are accelerated in the first half of the diode, decelerated in the second half, and finally leave the diode at their original (injection) velocity v_o. This behavior is consistent with the inference (from the end values of the electric field profile) that Q_{active} has a positive value in this final state.

Using the same characteristic second regime value of $\alpha = 1.5\pi$, the diode simulation was re-run, however this time with the original electrons bunched slightly towards the center; the resulting initial perturbation potential profile $\phi(x)$ is everywhere negative. Snapshots from early on in the resulting simulation ($t \lesssim 3$) again show the initial transit and adjustment (linear) stages. When these stages finish, the potential profile Fig. 10(a) is seen to approximate closely the theoretical prediction for the dominant eigenmode, Fig. 7(b); the potential profile extremum is again at $x = 0.37$, however in this negatively initialized run the sign of the recovered profile is now reversed compared with the previous, positively initialized case. As in the earlier case, the

dominant and next-to-dominant eigenfrequencies are most readily recovered from the external current diagnostic. Also as before, the dominant eigenmode stage is seen isolated for only a brief period ($2 \lesssim t \lesssim 4.5$) in the electrostatic energy history Fig. 11(a) and in the related energy growth rate diagnostic, Fig. 11(b).

Following these linear stages, the perturbation enters a nonlinear stage ($5 \lesssim t \lesssim 7$) in which the potential profiles Fig. 10(b) and (c) now differ from that recovered in the previous positively initialized run (Fig. 8). Also different in this run, the external current in the nonlinear stage is now decreasing in amplitude.

The diode continues to evolve nonlinearly, but this time it achieves a final state ($t \gtrsim 7$) that is periodic oscillatory (dynamic) instead of being d.c. as before.
These oscillations are especially visible in the external current $J_{ext}(t \gtrsim 7)$, Fig. 11(c), from which we find that they have a period very close to the plasma period of the original equilibrium medium.

In this final state, the potential profile, Fig. 12(a), has evolved from its early linear eigenmode profile into a more complicated shape involving an oscillating "virtual cathode" (a negative potential minimum ϕ_{min} near the injection plane, which oscillates in position and magnitude) between $x = 0.08$ and $x = 0.22$. This virtual cathode differs substantially from the nearly parabolic shape recovered as the final state in the pre-

dominant and next-to-dominant eigenfrequencies are most readily recovered from the external current diagnostic. Also as before, the dominant eigenmode stage is seen isolated for only a brief period ($2 \lesssim t \lesssim 4.5$) in the electrostatic energy history Fig. 11(a) and in the related energy growth rate diagnostic, Fig. 11(b).

Following these linear stages, the perturbation enters a nonlinear stage ($5 \lesssim t \lesssim 7$) in which the potential profiles Fig. 10(b) and (c) now differ from that recovered in the previous positively initialized run (Fig. 8). Also different in this run, the external current in the nonlinear stage is now decreasing in amplitude.

The diode continues to evolve nonlinearly, but this time it achieves a final state ($t \gtrsim 7$) that is periodic oscillatory (dynamic) instead of being d.c. as before.
These oscillations are especially visible in the external current $J_{ext}(t \gtrsim 7)$, Fig. 11(c), from which we find that they have a period very close to the plasma period of the original equilibrium medium.

In this final state, the potential profile, Fig. 12(a), has evolved from its early linear eigenmode profile into a more complicated shape involving an oscillating "virtual cathode" (a negative potential minimum ϕ_{min} near the injection plane, which oscillates in position and magnitude) between $x = 0.08$ and $x = 0.22$. This virtual cathode differs substantially from the nearly parabolic shape recovered as the final state in the pre-

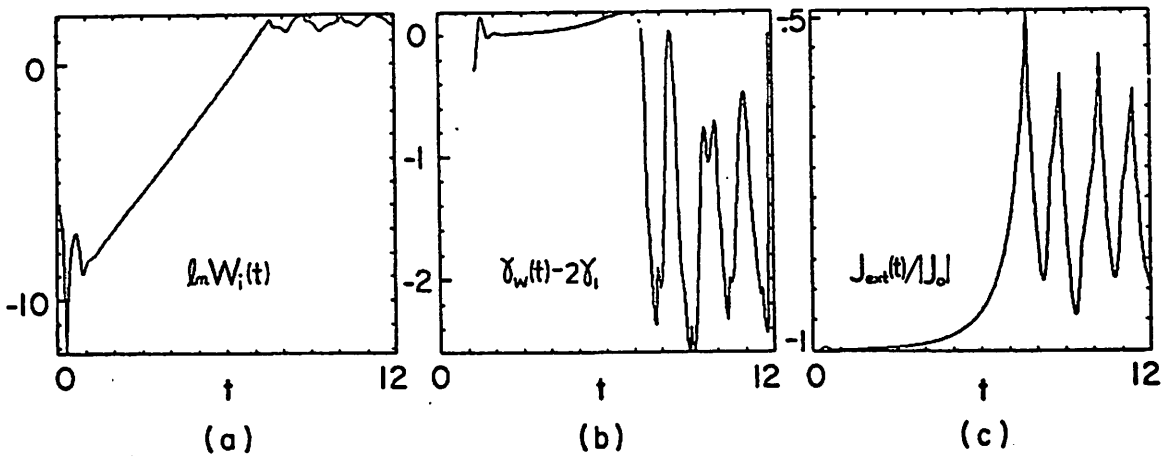

Figure 11. Case: $\alpha = 1.5\pi$, negative initialization. History plots showing (a) the internal electrostatic energy, $\ln W_i(t)$, and (b) the difference between the simulation energy rate of change, $\gamma_W(t)$, and the predicted growth rate in the dominant eigenmode stage, $2\gamma_1$ (not evaluated for $t < 1$ to avoid "initial transit" stage), and (c) external current $J_{ext}(t)/|J_o|$.

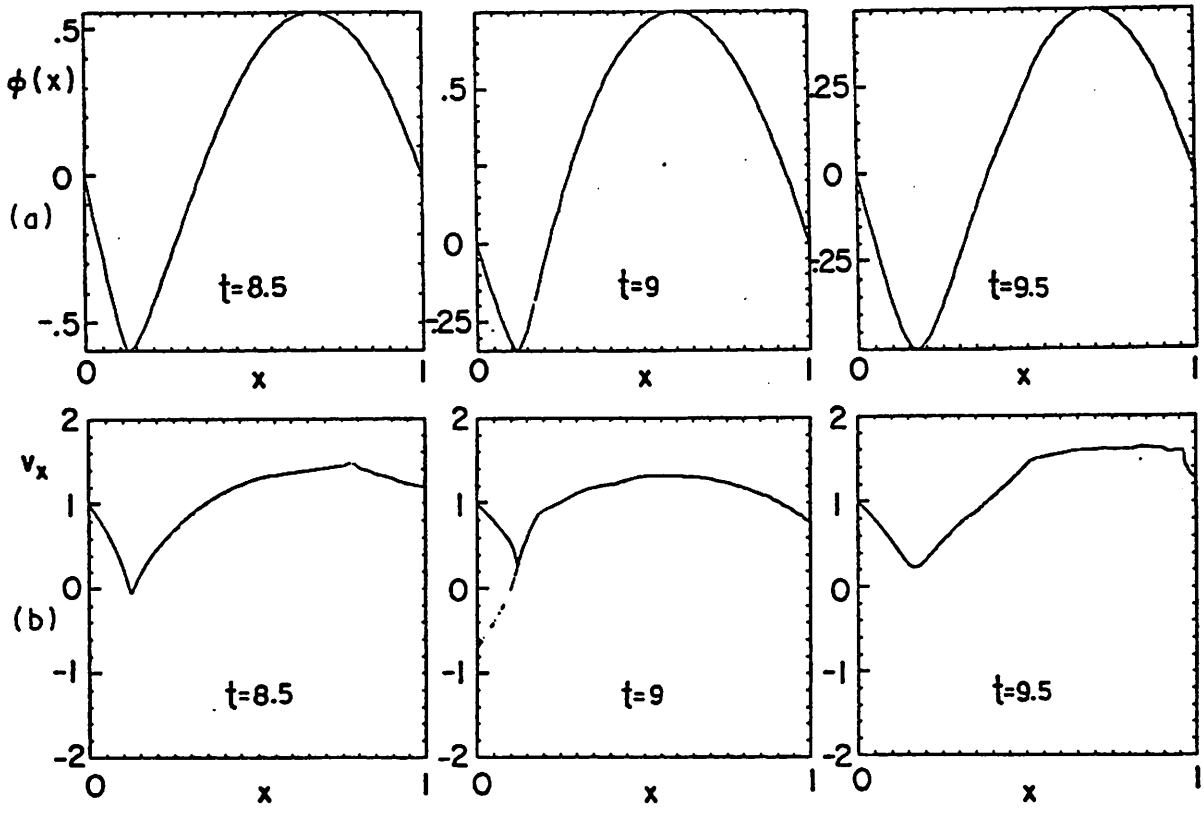

Figure 12. Case: $\alpha = 1.5\pi$, negative initialization. Final state nonlinear behavior of the Pierce diode. Snapshots show diode at t = 8.5, 9, and 9.5. (a) Potential profiles $\phi(x)$, and (b) the corresponding electron phase spaces; samples are spread through one oscillation period.

vious case of positive initialization. The net space charge profile $\varrho(x)$ also has a well defined extremum at the position of the virtual cathode, with corresponding oscillations in position.

The electron phase space in this nonlinear final stage is dynamic, clearly never reaching a time independent (steady) state. Severe distortions occur in the beam, especially near the cathode where newly injected electrons quickly feel the strongly depressed potential minimum and are decelerated, thereby building up the diode total charge. In this oscillatory final state, the net charge contained between the plates, $Q_{active}(t)$, is always negative (the diode is electron rich) and oscillates with the same period as $J_{ext}(t)$. When ϕ_{min} falls below -0.5 (the electron injection energy), then new electrons are reflected back to the injection plane where they are absorbed; at such times, the electron velocities are clearly not single valued and the ensemble can thus no longer be collectively described as a simple "fluid". When such complete reflection occurs, charges are leaving the diode at both ends and Q_{active} quickly relaxes from its built up value, allowing free entry to the injected electrons once again. This periodic reflection of electrons to the cathode and the following rapid change in Q_{active} accounts for the large, relaxation type (nosinusoidal) oscillations seen in both $W_i(t)$ and $J_{ext}(t)$, Fig. 11(a) and (c). The significant

vious case of positive initialization. The net space charge profile $\varrho(x)$ also has a well defined extremum at the position of the virtual cathode, with corresponding oscillations in position.

The electron phase space in this nonlinear final stage is dynamic, clearly never reaching a time independent (steady) state. Severe distortions occur in the beam, especially near the cathode where newly injected electrons quickly feel the strongly depressed potential minimum and are decelerated, thereby building up the diode total charge. In this oscillatory final state, the net charge contained between the plates, $Q_{active}(t)$, is always negative (the diode is electron rich) and oscillates with the same period as $J_{ext}(t)$. When ϕ_{min} falls below -0.5 (the electron injection energy), then new electrons are reflected back to the injection plane where they are absorbed; at such times, the electron velocities are clearly not single valued and the ensemble can thus no longer be collectively described as a simple "fluid". When such complete reflection occurs, charges are leaving the diode at both ends and Q_{active} quickly relaxes from its built up value, allowing free entry to the injected electrons once again. This periodic reflection of electrons to the cathode and the following rapid change in Q_{active} accounts for the large, relaxation type (nosinusoidal) oscillations seen in both $W_i(t)$ and $J_{ext}(t)$, Fig. 11(a) and (c). The significant

decrease in the average value of $J_{ext}(t)$ (some 25% smaller than J_o in the final state) is a measure of the net return of injected electrons back to the cathode.

To conclude, our particle simulations again recover predicted linear behavior of the Pierce diode operating in the unstable, purely growing, second α-regime. Both the dominant (purely growing, positive imaginary) and the next-to-dominant (damped oscillating, complex with negative imaginary part) eigenfrequencies are recovered. The linear character of the diode is consistent with that found for the first (stable) α-regime: When the sign of the initialization is reversed, the eigenfrequencies of the diode are found to be unchanged, while the eigenmode profiles recovered have the same shape but are changed in sign. The final (nonlinear) state of the diode, however, depends critically on the initial condition sign: With a positive initial potential profile, the linear growth saturates to a new time independent equilibrium (steady state) having a positive, nearly parabolic potential profile; in reaching this new equilibirium, the external current first increases by nearly a factor of two before relaxing back to its constant (electron injection) value, $J_{ext}(t\rightarrow\infty) = J_o$. With a negative initial potential profile, the linear growth leads to a final state having large amplitude, relaxation oscillations, both internally and externally; the potential profile shows an oscillating virtual

cathode; the corresponding electron phase space shows electrons being returned periodically to the cathode; the external current exhibits the large oscillations along with a decrease in its time average of roughly 25% below its d.c. injection value.

cathode; the corresponding electron phase space shows electrons being returned periodically to the cathode; the external current exhibits the large oscillations along with a decrease in its time average of roughly 25% below its d.c. injection value.

IV. THIRD REGIME: $2\pi < \alpha < 3\pi$

Analysis:

In the third α-regime, the Pierce characteristic relation (1) finally returns oscillatory instabilities in that the dominant eigenfrequency is now fully complex, having both a non-zero real part and a positive imaginary part. Once again, the linear response is expected[5] to have initial-transit and adjustment stages before we can clearly see the dominant eigenmode. After a period of dominant-eigenmode growth, the diode should again evolve nonlinearly into its final state.

For a representative value $\alpha = 2.5\pi$, the complex dominant eigenfrequency is calculated[5] from the characteristic equation (1) to be $\omega_1/\omega_p = 0.1819 + 0.0750i$; the next-to-dominant eigenfrequency is $\omega_2/\omega_p = 1.9203 - 0.3748i$. Because the dominant eigenfrequency is fully complex, the corresponding eigenmode spatial profile is now also complex i.e., there are two component profiles[5] (corresponding to the real and imaginary parts) for each of $\phi(x)$ and $E(x)$. For example, the theoretical dominant eigenmode potential profile has a form (to within a phase constant)

$$\begin{aligned}\phi(x,t) &= \mathrm{Re}\left\{\left[\phi_r(x)+i\phi_i(x)\right]e^{-i\omega_1 t}\right\} \\ &= \left[\phi_r(x)\cos\omega_{1r}t+\phi_i(x)\sin\omega_{1r}t\right]e^{\gamma_1 t}.\end{aligned} \tag{6}$$

The calculated real and imaginary component profiles[5] are as shown in Fig. 13 for both the electric field $\bar{E}(x)$ and the potential $\phi(x)$.

Simulations:

A particle simulation for the case $\alpha = 2.5\pi$ is initialized with perturbed $\varrho(x)$ such that $\phi(x)$ is everywhere positive (simlar to Fig. 3).

Because in this α-regime the top two eigenfrequencies are both fully complex, subtracting out the dominant during the early linear stages to uncover the next-to-dominant is no longer as straightforward as it was in the lower α-regimes. For $t \lesssim 1.1$ the internal electrostatic energy history Fig. 14(a) is too thoroughly contaminated with transients to reasonably extract even Re ω_2. The external perturbation current Fig. 14(b) shows weaker transients than does the internal energy, but the simple frequency diagnostic[12] can still only resolve that $1.6 \lesssim \text{Re}\,\omega_2/\omega_p \lesssim 2.2$, in reasonable (but not conclusive) agreement with the real part of the expected next-to-dominant given above.

In the dominant eigenmode stage ($1.5 \lesssim t \lesssim 6$), the internal energy $W_i(t)$ exhibits constant, oscillatory growth in which the dominant eigenfrequency can readily be discerned; from this diagnostic it is measured to be $\omega_1/\omega_p = 0.184 + 0.075i$. Corresponding oscillations are seen

The calculated real and imaginary component profiles[5] are as shown in Fig. 13 for both the electric field $\vec{E}(x)$ and the potential $\phi(x)$.

Simulations:

A particle simulation for the case $\alpha = 2.5\pi$ is initialized with perturbed $\varrho(x)$ such that $\phi(x)$ is everywhere positive (simlar to Fig. 3).

Because in this α-regime the top two eigenfrequencies are both fully complex, subtracting out the dominant during the early linear stages to uncover the next-to-dominant is no longer as straightforward as it was in the lower α-regimes. For $t \lesssim 1.1$ the internal electrostatic energy history Fig. 14(a) is too thoroughly contaminated with transients to reasonably extract even Re ω_2. The external perturbation current Fig. 14(b) shows weaker transients than does the internal energy, but the simple frequency diagnostic[12] can still only resolve that $1.6 \lesssim \text{Re}\ \omega_2/\omega_p \lesssim 2.2$, in reasonable (but not conclusive) agreement with the real part of the expected next-to-dominant given above.

In the dominant eigenmode stage ($1.5 \lesssim t \lesssim 6$), the internal energy $W_i(t)$ exhibits constant, oscillatory growth in which the dominant eigenfrequency can readily be discerned; from this diagnostic it is measured to be $\omega_1/\omega_p = 0.184 + 0.075i$. Corresponding oscillations are seen

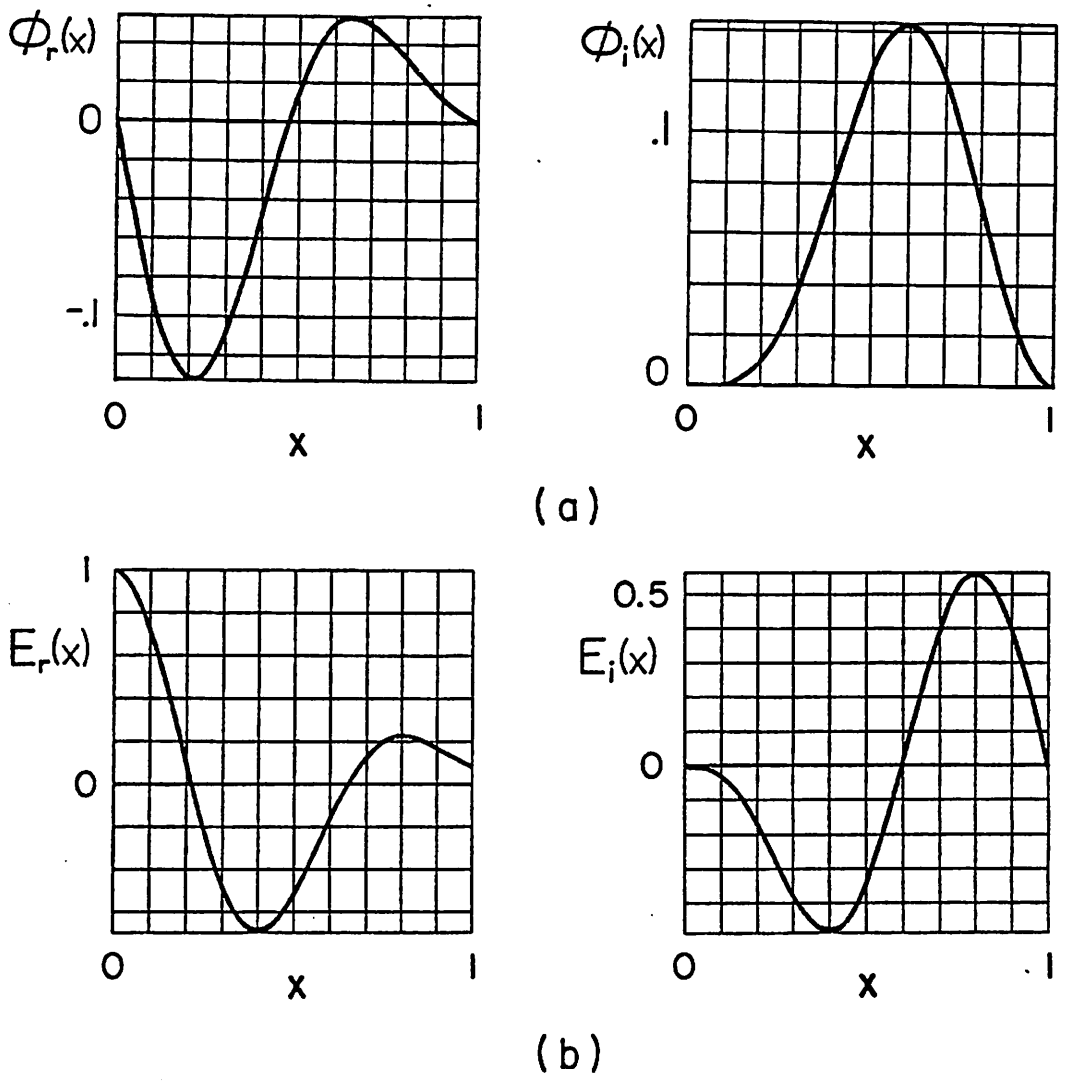

Figure 13. Case: $\alpha = 2.5\pi$. Calculated linear dominant eigenmode profiles. (a) "Real" and "imaginary" potential profiles, and (b) corresponding electric field components.

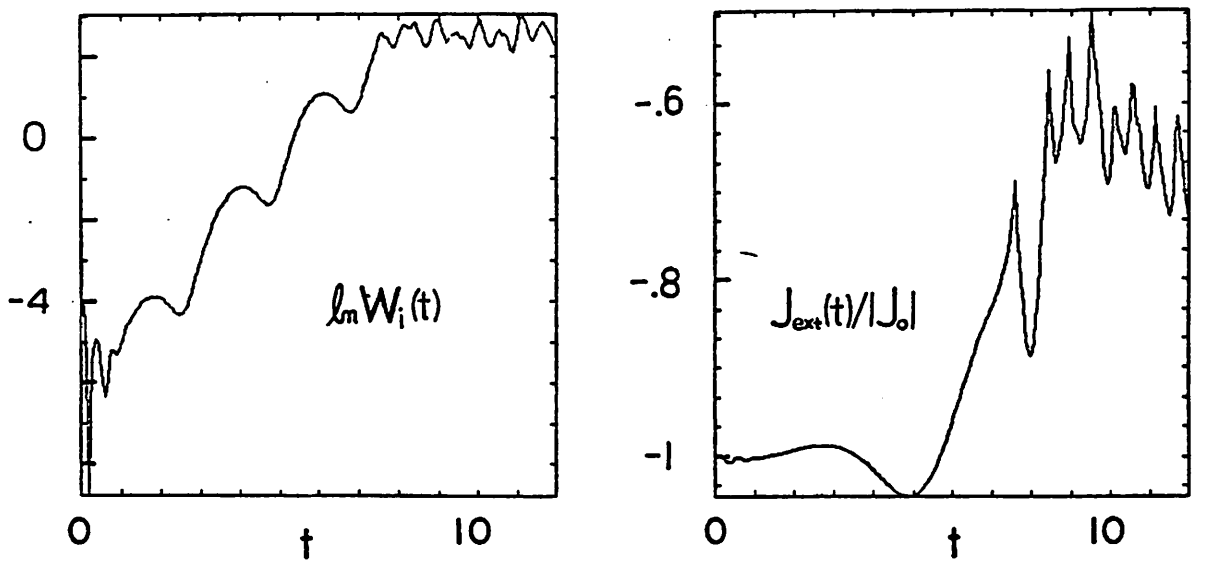

Figure 14. Case: $\alpha = 2.5\pi$, negative initialization. History plots showing (a) system internal electrostatic energy, $\ln W_i(t)$, and (b) external circuit current, $J_{ext}(t)/|J_o|$.

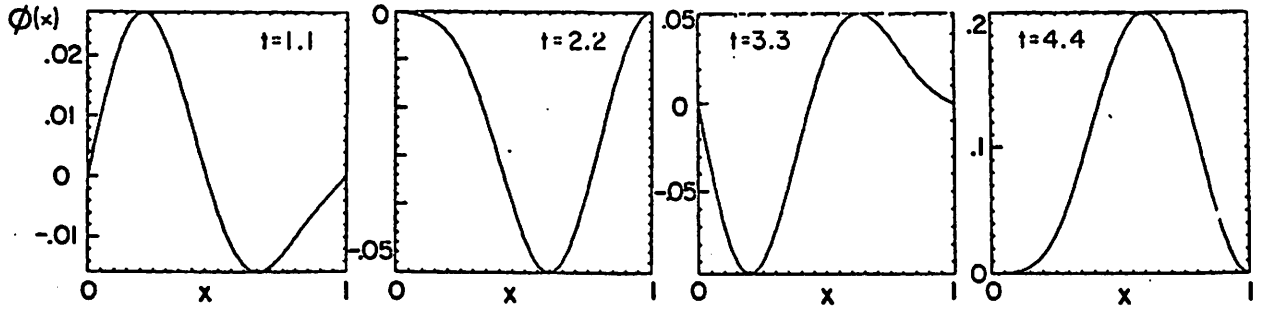

Figure 15. Case: $\alpha = 2.5\pi$, positive initialization. Dominant eigenmode stage oscillations in the potential profile, shown at quarter-period intervals. The shapes agree with the theoretical eigenmode predictions (Fig. 13) while their amplitudes are growing exponentially (Fig. 14(a)).

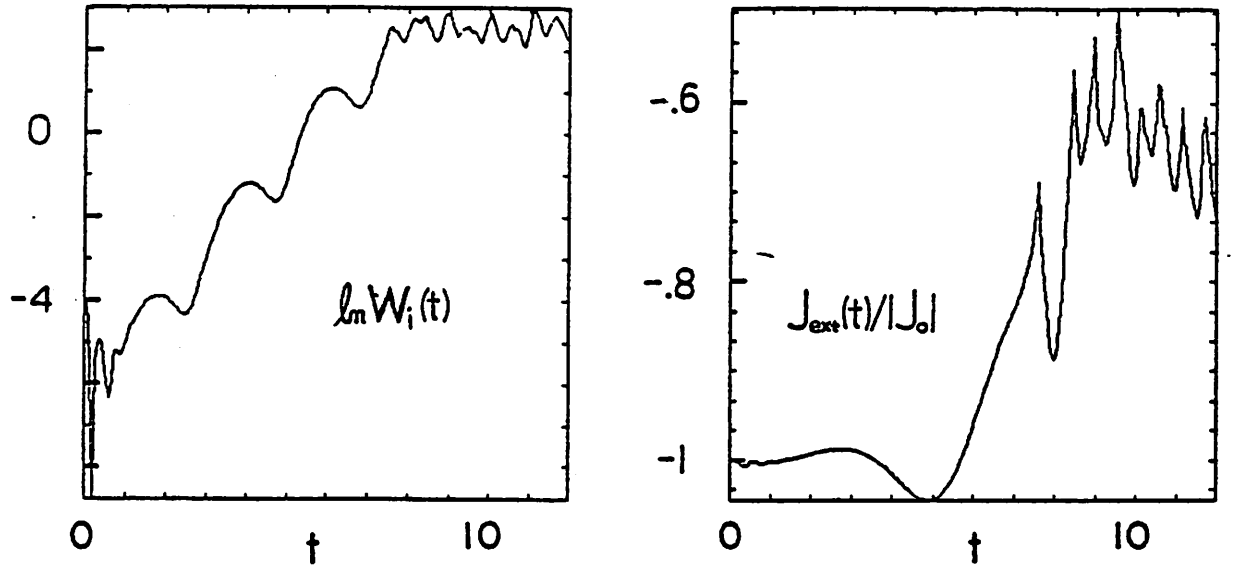

Figure 14. Case: $\alpha = 2.5\pi$, negative initialization. History plots showing (a) system internal electrostatic energy, $\ln W_i(t)$, and (b) external circuit current, $J_{ext}(t)/|J_o|$.

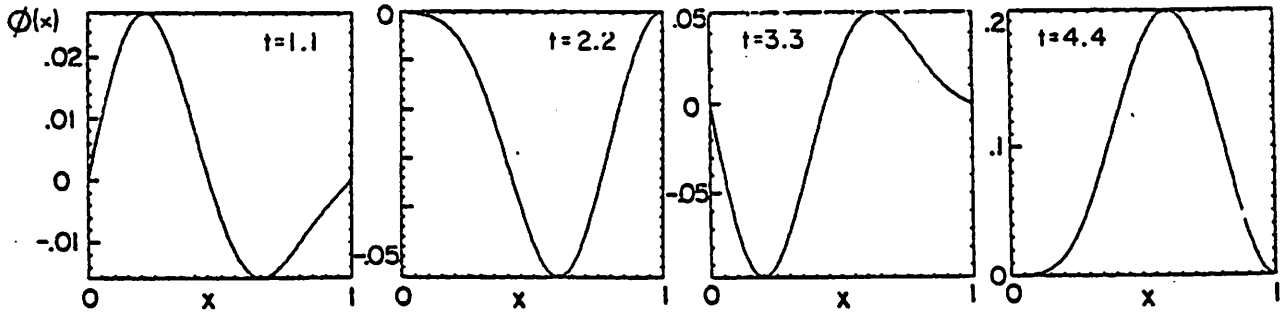

Figure 15. Case: $\alpha = 2.5\pi$, positive initialization. Dominant eigenmode stage oscillations in the potential profile, shown at quarter-period intervals. The shapes agree with the theoretical eigenmode predictions (Fig. 13) while their amplitudes are growing exponentially (Fig. 14(a)).

in $Q_{active}(t)$ during which the total charge in fact changes sign. As additional verification that the dominant eigenmode is recovered, snapshots of $\phi(x)$ were made for $t > 1.1$; as shown in Fig. 15, at quarter periods of ω_{1r} the simulation potential profiles are seen to agree very closely with the predicted real and imaginary profiles of Fig. 13(a). The same linear profile results (however with opposite sign) were also recovered in a companion run which had a negative initial potential profile.

Beyond the linear response, $t \gtrsim 7$, a nonlinear final state develops which shows "noisy" oscillations, both internally in $W_i(t)$ and externally in the current. The time average of $J_{ext}(t)$ has now been reduced roughly 30% indicating substantial reflection of the injected electrons back to the cathode. By the end of our simulation run, the electron phase space Fig. 16 has achieved a correspondingly noisy final condition. Although we did not run the simulation beyond $t = 12$, it is reasonable to expect that subsequent evolution of the system affects only the detailed structure of the electron phase space, without significant modification of the electrostatics.

Qualitatively very similar linear and final states are also recovered for negatively initialized runs.

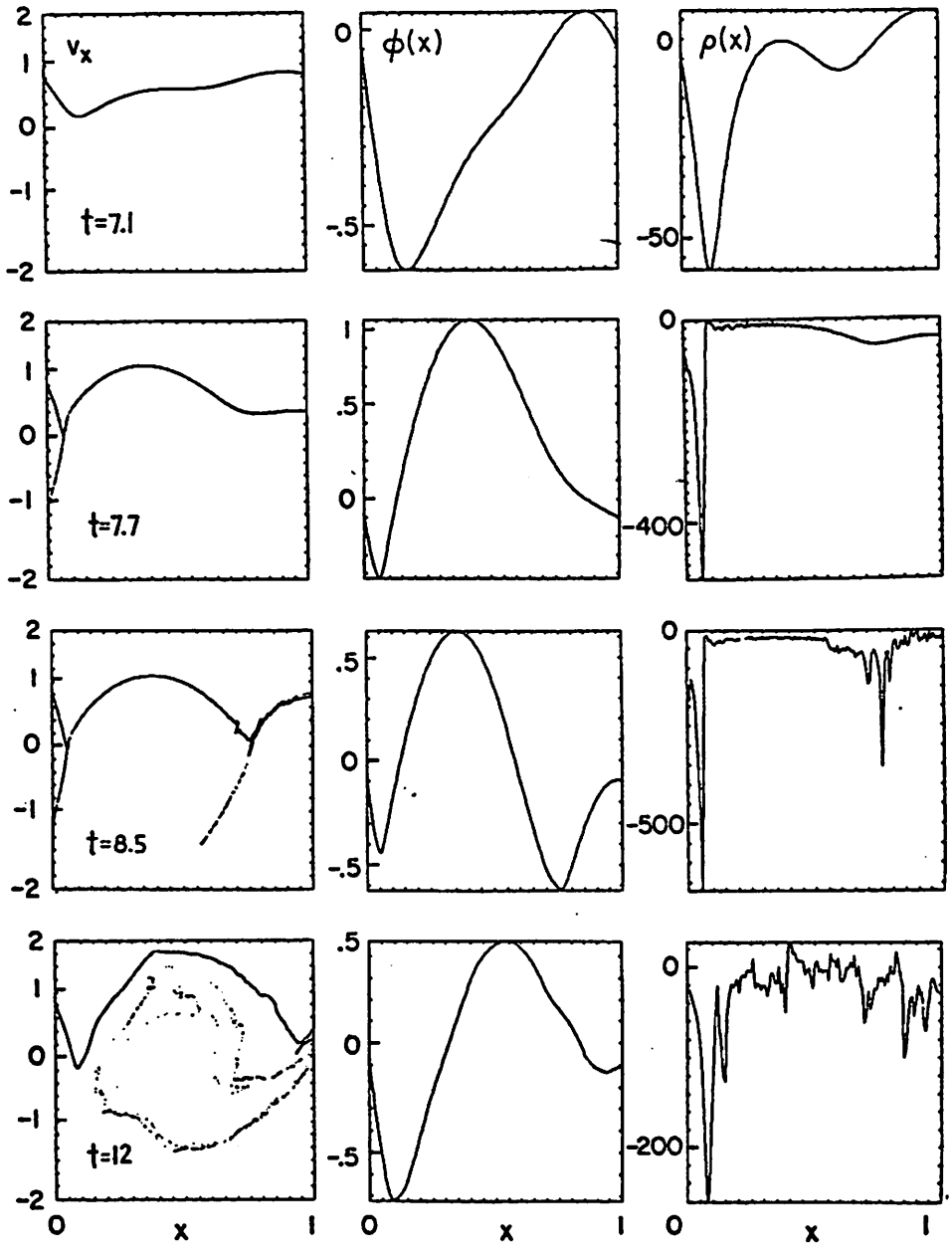

Figure 16. Case: $\alpha = 2.5\pi$, positive initialization. Nonlinear diode behavior from shortly after dominant eigenmode stage, t = 7.1, to effective final state at t=12. Electron phase space, potential profiles, and spatial charge density showing virtual cathode.

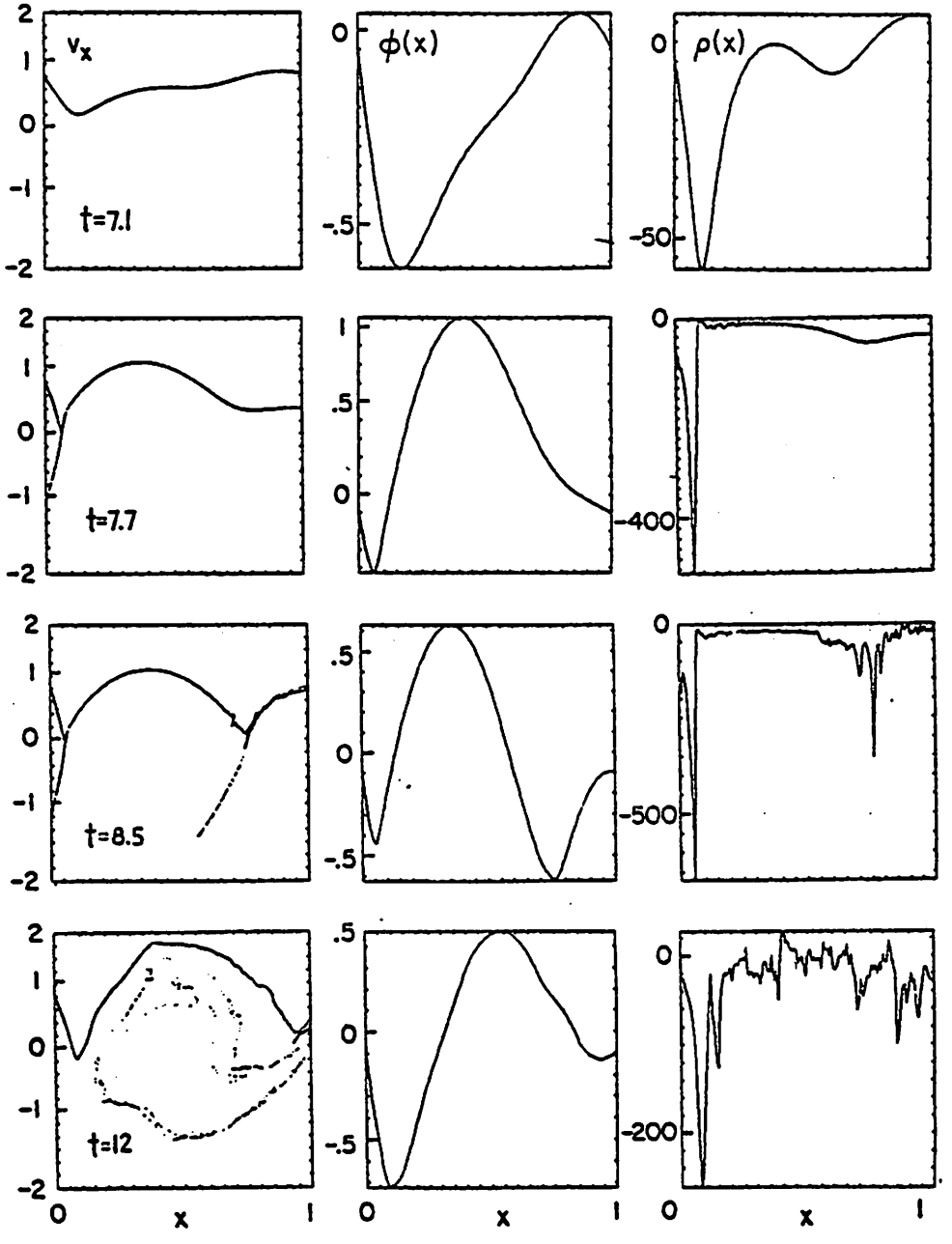

Figure 16. Case: $\alpha = 2.5\pi$, positive initialization. Nonlinear diode behavior from shortly after dominant eigenmode stage, t = 7.1, to effective final state at t=12. Electron phase space, potential profiles, and spatial charge density showing virtual cathode.

V. DISCUSSION AND CONCLUSIONS

Particle simulations of the uniform classical Pierce diode in the low-α regimes $0 < \alpha < 3\pi$ have successfully recovered predicted[5] linear behavior (i.e., frequencies and mode profiles) of the top eigenmodes. These simulations confirm the system's different stability characteristics, depending simply on the single free parameter $\alpha = \omega_p L/v_o$. Considering a fixed length system and an electron injection scheme that operates at a constant velocity, this parameter α is then interpretable as injected current density. For small enough injection current ($\alpha < \pi$), the diode is stable.

When the current injection is large enough to make the system unstable, our simulations follow an initial perturbation in the diode as the linear response stages evolve into nonlinear. Eventually a final state is reached. The character of this final state can depend critically on the initial conditions: in the second α-regime ($\alpha = 1.5\pi$), depending simply on the sign of the initial perturbation potential, the diode either reaches a new non-classical, time independent equilibrium (positive initialization) or it develops large amplitude, periodic, relaxation type oscillations (negative initialization).

ACKNOWLEDGMENTS

We are indebted to Prof. C.K. Birdsall for stimulating discussions, and to Mr. Wm.S. Lawson for his major contribution to the code PDW1. This work was performed under DOE Contract DE-AT03-76ET53064 and ONR Contract N00014-77-C-0578. The second author acknowledges partial support from the Austrian Scientific Research Funds under Contracts S-18/03 and P5178. The computations were all done at the National Magnetic Fusion Energy Computer Center, Livermore, CA.

ACKNOWLEDGMENTS

We are indebted to Prof. C.K. Birdsall for stimulating discussions, and to Mr. Wm.S. Lawson for his major contribution to the code PDW1. This work was performed under DOE Contract DE-AT03-76ET53064 and ONR Contract N00014-77-C-0578. The second author acknowledges partial support from the Austrian Scientific Research Funds under Contracts S-18/03 and P5178. The computations were all done at the National Magnetic Fusion Energy Computer Center, Livermore, CA.

[1]J.R. Pierce, J.Appl.Phys. 15, 721 (1944).

[2]J. Frey and C.K. Birdsall, J.Appl.Phys. 36, 2962 (1965).

[3]J.R. Cary and D.S. Lemons, J.Appl.Phys. 53, 3303 (1982).

[4]B.B. Godfrey, Mission Research Corporation, Report Nos. AMRC-R-282, 1981, AMRC-N-212, 1982, and AMRC-N-245, 1983.

[5]S. Kuhn, Phys.Fluids 27, 1834 (1984).

[6]Wm.S.Lawson, Electronics Research Laboratory, U.C. Berkeley, PDW1 User's Manual, Memorandum No. UCB/ERL M84/37, 1984.

[7]N. Rostoker and M. Reiser (eds.), Collective Methods of Acceleration (Harwood, 1979).

[8]D.S. Lemons and J.R. Cary, J.Appl.Phys. 53, 4093 (1982).

[9]S. Kuhn, Phys.Rev.Lett. 50, 217 (1983).

[10]E.A. Coutsias and D.J. Sullivan, Phys.Rev.A 27, 27 (1983).

[11]N.A. Krall and A.W. Trivelpiece, Principles of Plasma Physics (McGraw-Hill, 1973).

[12]O. Buneman, J.Comp.Phys. 29, 295 (1978).